Developing a Mechanistic Model for Flow through a Perforated Plate with Application to Screening of Particulate Materials

Olumide Ogunmodimu

B.Sc.(Hons), Bowen University, Iwo, Nigeria 2008

MSc, University of Cape Town, South Africa 2013

Supervisors

Prof. Aubrey Mainza, Prof. Indresan Govender, Prof. J-P Franzidis

Thesis presented for the degree of

DOCTOR OF PHILOSOPHY

in the Department of Chemical Engineering

UNIVERSITY OF CAPE TOWN

October 2016

University of Cape Town

The copyright of this thesis vests in the author. No quotation from it or information derived from it is to be published without full acknowledgement of the source. The thesis is to be used for private study or non-commercial research purposes only.

Published by the University of Cape Town (UCT) in terms of the non-exclusive license granted to UCT by the author.

University of Cape Town

Abstract

Screening in mineral processing is the practice of separating granulated ore materials into multiple particle size fractions, and is employed in most mineral processing plants. Models of screening performance have been developed previously with the aim of improving process efficiency. Different methods have been used, such as physical modelling, empirical modelling, and mathematical modelling including the discrete element method (DEM). These methods have major limitations in practice, and experimental data to validate the models have been difficult to obtain. Currently, the design and scale-up of screens still relies on rules of thumb and empirical factor methods rather than a fundamentally based understanding of the behaviour of the granular system.

To go beyond the current state-of-the-art in screen modelling requires a clear understanding of the particle motion along a dynamic (vibrating) inclined plane. Central to this understanding is the notion that granular systems exhibit a unique rheology that is not observed in fluids; i.e. neither Newtonian nor non-Newtonian. It is thus imperative to fully quantify the granular rheology, which is determined by the depth of the particle bed along the screen, the solids concentration, and the average velocity of the granular avalanche on the screen. The concept of granular rheology is important. Existing empirical models of vibrating screens tend to be extremely dependent on boundary conditions of a particular machine design. The concept of granular rheology is important because, akin to fluid flow, granular flow exhibits different flow regimes depending on the extent of energy input in the system.

This work employed DEM to quantify the granular rheology of particles moving along a vibrating inclined screen in order to begin the development of a phenomenological model of screening. The model extends the visco-plastic rheology formation of Pouliquen et al. (2006) to capture the kinetic and turbulent stresses obtained in granular flow on an inclined vibrating screen. In general, DEM was employed to develop a mechanistic model of screening which includes a description of the rheology of granular flow on a vibrating screen. Microscopic properties of granular flow were used in DEM to simulate screening of particulate materials. Granular mixtures of two particle constituents (3 mm and 5 mm) were simulated on an inclined vibrating screen of 3.5 mm apertures. For the base case, frequency and amplitude are 4 Hz and 1 mm, respectively. While microscopic properties were employed for the simulation, the properties extracted from the simulations are macroscopic fields which are consistent with the continuum equations of mass, momentum and energy balance. From the continuum equations, a micro-macro transition method called the coarse-graining approach was employed to obtain the volume fraction and the tangential velocity as a function of the depth of flow along the inclined surface.

This approach is suitable for this work because the produced fields satisfy the equations of continuum mechanics; even near the base of the flow. The continuum analysis of the flowing layer reveals a coexistence of flow regimes- (i) quasi-static, (ii) dense (liquid-like), and (iii) inertial. The regimes are consistent with the measured solids concentrations spanning these regimes on inclined vibrating screens. The quasi-static regime is dominated by frictional stress and corresponds to low inertial number (I). Beyond the quasi-static regime, the frictional

stress chains break and the collisional-kinetic and turbulent stress begin to dominate.

The variation of the effective frictional coefficient with the inertial number (I) characterises the flow. Finally, an effective frictional coefficient model that is based on frictional, collisional-kinetic and turbulent stress was developed. Data analyses for this model were done at a steady flow in the base case where a coexistence of three flow regimes were observed. It was observed that each regime of flow is dominated by corresponding shear stresses. While the quasi-static regime is dominated by frictional stress, the kinetic and the inertial regimes are dominated by kinetic and turbulent shear stresses, respectively. This model was tested by varying the intensity of vibration in the base case and it was observed that at higher frequencies and amplitudes, the quasi-static regime gradually disappeared. Furthermore, the inertial number at which transition occurs to different regimes varies in response to the intensity of vibration.

This is an important step in developing a phenomenological model of screening. The model presents a fundamental understanding of the mechanisms governing transport of granular matter on an inclined vibrating screen.

Statement of Originality

In granular flow research, a single rheological description of the flow on a vibrating screen has not yet been realised. There has been some progress towards the development of a complete theory describing the behaviour of granular flow along an inclined plane geometry. Many of models of vibrating screens are empirically based, and tend to be extremely dependent on boundary conditions of a particular machine design. This makes it difficult to extrapolate empirical models beyond their specific design. This work uses the physics of particle interactions to model the mechanisms of granular dynamics on an inclined vibrating screen. In order to construct a unifying rheological model that captures the main features of granular flow on a vibrating screen, this work develops a constitutive stress model that captures all the known stresses in the flow and the transitions between the known flow regimes.

Analysis of the shear and normal stresses in the different regimes of flow shows the dominant stress and energy dissipation in the system. Discrete particle simulation data were extracted to provide the required closure rules for the rheological model to characterise the granular flow on a vibrating inclined screen. The discrete particle data were analysed with the coarse graining average method to find the continuum fields (of average velocity, volume fraction, and scaled depth of flow from the continuum equations of mass, momentum and energy balance). Similar to the Bagnold profile,there is a relationship between the average velocity and the depth of flow. At steady state, the average velocity of the flow varies as the scaled depth in the form, $\langle V \rangle \propto (h/d)^n$, where $n = 0.4017$. The model developed in this work reveals that granular flow on an inclined vibrating screen exhibits different flow regimes and the observed three regimes, quasi-static, kinetic and turbulent were successfully captured by a rheological mesoscopic model.

Declaration

I hereby declare that the work in this document is expressed in my own words. The use of other author's ideas, equations or expressions in any form within this work is properly acknowledged. The document contains a list of references employed in this study.

.....

Olumide O OGUNMODIMU

Dedication

Unto God Almighty the giver of wisdom, from whose mouth comes knowledge and understanding. I will sing of His mercies forever.

Acknowledgements

I owe the successful completion of this work to God almighty the giver of wisdom and life. A journey of this sort could only have been made possible by His grace and the kindness of people He sent to assist me throughout the duration of my research. My thanks and appreciation to my supervisors Prof. Indresan Govender, Prof. Aubrey Mainza and Prof J-P Franzidis for persevering with me as my advisors throughout the time it took me to complete my research and write the dissertation. It has been an honour to work under the supervision of these great scholars. Your patience, tolerance and passion to impact knowledge is unparalleled. Accomplishing this work would have been difficult without their financial supports, insightful critiques, contributions and provision of necessary materials as and when needed.

I have to register my profound appreciation to the South African Minerals to Metals Research Institute (SAMMRI) and UCT Postgraduate Funding Office for the funding and support for this project. Special thanks to the Minerals to Metals Initiative, Department of Chemical Engineering UCT for the opportunity given me to learn. I benefited both financially and intellectually from this department, for this I am grateful.

I am as well grateful to Dr. Lawrence Bbosa, Dr. Kathryn Cole and Mr David de Klerk for their contributions and their good-natured support. I am grateful to many persons who shared their experiences and memories especially the RCF-UCT family, my egbons Dr Seun & Mrs Toke Oyekola, Dr Femi & Mrs Wumi Olaofe, Dr Niyi & Mrs Wumi Isafiade, my friend Dr Femi Olaoye and my flatmate Dr Edmund Okoroigwe. I will also like to appreciate the following persons whose help and encouragement have been of great significance: Aderonke Ajayi-smith, Abigail, Prisca, Pelumi, Opeyemi, Omodanisi Ife, Ayodele Periola, Ayodele Ogunkoya, Abikoye Ben, Jude Bonsu and the rccg family in Cape Town. My thanks also to my friends at the Energy Research Centre (ERC-UCT); Fadiel Ahjum, Michael Boulle and Bryce McCall.

I must acknowledge as well the many friends and colleagues, lecturers, students, and everyone who assisted, advised and supported my research and writing efforts over the years. Especially, I want to express my deep appreciation to Dr Ikena & Mrs Rosemary Ireka, the family of Wilson & Aderonke Sakpere, the family of Lanre & Titi Kunuji and the family of Seun & Tejumade Ogundipe whose friendship, hospitality, prayers and support have helped me over the years of our friendship and are difficult to quantify. A special thanks is also extended to Pastor and Mommy Adelusi for their love and encouragement. My thanks must go to my dear friend Tolulope Fadina for keeping faith with me all these years, your support and encouragement is deeply appreciated.

Finally, and certainly not the least, I want to specially appreciate my family, my parents - Chief E. Bayo Ogunmodimu and Mrs Funmilayo Ogunmodimu for their parental care, prayers, financial and emotional support. Daddy and Mommy, I owe you a big thank-you and couldn't have made it but for your unconditional love. Furthermore, I cannot but appreciate my siblings - Morakinyo & Toni Ogunmmodimu, Gbenga & Toyin Ogunmodimu, Bunmi Vincent, Kunle & Similoluwa Adeyanju, Olayinka, Monisola, Wale, Ope, Bisi Nwabuikwu, Mogbonjubola, Toyin and Bukola. For your numerous supports and encouragement I say a big thank you.

Contents

List of Figures

List of Tables

Chapter 1

Introduction

1.1 Background

The purpose of this thesis is to take a first step towards developing a phenomenological model of screening by studying the rheology of granular flow on an inclined vibrating screen. Screening is the most widespread method of sizing in mineral processing, and vibrating screens are among the most common types of screens used to separate particles into different size fractions. Screens are efficient at coarse sizes but become inefficient when applied to the separation of fine materials. Due to their versatility in minerals processing, improving efficiencies at the fine end would lead to better capacities per defined screen area which would result in significant economic benefits.

Improved screening efficiencies would also have a positive effect on downstream separation efficiencies as more particles are delivered with the preferred properties to the separation section. In a bid to reduce the use of energy through less over-grinding, new technologies such as Landsky and Derrick screens have made significant improvements to fine screening (Mainza et al. 2004; Makinde et al. 2015; Mainza et al. 2013). However, understanding the rheology of granular flow would, in the long term, lead to an accurate and rapid design of screening systems. The major beneficiaries of these improvements would likely be industries

where large volumes of particles are screened, such as the aggregate in diamond, iron ore, copper, platinum, gold and coal industries.

There is no doubt that screening models based on the mechanisms of classification would lead to improved screening efficiencies. However, although simple in concept, the modelling of screen performance for better efficiency is not trivial. Much work has been done to examine the basic factors that influence the performance of screens, but not to the point of developing mechanistic models able to predict the efficiency of industrial screens accurately (Grozubinsky et al. 1998; Kruggel-Emden and Elskamp 2014). Currently, the design and scale-up of screens still rely on rules of thumb and methods involving many empirical factors. While studies in the past used only empirical data for their analyses (Tsakalakis 2001; Apling 1984; Ferrara et al. 1988) more recent studies have employed both empirical data and Discrete Element Method (DEM) modelling to validate their results (Kruggel-Emden and Elskamp 2014; Hilden 2007; Mainza et al. 2013). These analyses are generally limited to studying the effect of different operating parameters on the efficiency of screens, although in some cases models are developed to calculate the efficiency of specific systems. However, these models are not generic in application as they cannot predict the efficiency of screens *a priori*.

To go beyond the current state-of-the-art in screen modelling requires a clear understanding of the particle motion along a dynamic (vibrating) inclined plane. Central to this understanding is the unique rheology that granular systems exhibit in screening: a rheology that is not akin to fluids - i.e., it is neither Newtonian nor non-Newtonian. Granular materials can be described as macroscopic, discrete solid particles such as sand, stones, glass beads, food grains etc. They are processed in vast quantities in nature and are second only to water as the most handled material in industry. Understanding granular flow is difficult as this highly dissipative system can behave as a solid, liquid or gas depending on the extent of energy input: thus, there is no unify governing equation yet established, like the Navier-Stokes equation in classical fluid flow, to capture all the observed behaviour of granular matter.

Indeed, the number of properties of granular flow obfuscate the use of continuum thermo- and hydro-dynamical principles (Holyoake 2012). Unlike fluid flow, granular flow exhibits negligible thermal fluctuations; hence, there is no classical fluctuation-dissipation theorem to predict the behaviour of a granular system. Moreover, because of the highly dissipative interactions in granular systems, kinetic theory fails as particles are not in constant random motion. In addition, a lack of clear separation between the microscopic grain scale and the macroscopic flow scale means that continuum models often cannot capture important regions where there is thin flow (Holyoake 2012), or where, at critical densities, jamming occurs (i.e when particles become rigid with increasing density).

Further to these basic problems associated with granular flow, granular systems exhibit a range of complex phenomena such as mixing, segregation and percolation, especially systems comprising particles of different sizes and densities (Yang et al. 2008). Segregation and percolation are crucial to the size separation of particulate materials in mineral processing. Sieves and screens are used both in industry and in the laboratory for particle size classification: screening is most often used for continuous sizing operations, while sieving is usually a batch operation. While segregation and percolation are known to cause numerous problems in granular dynamics, for instance in the food and pharmaceutical industries (Prescott and Carson 2000), they are an advantage in screening.

The question as to whether a single set of constitutive relations will capture the wide spectrum of granular behaviour remains open to physicists and engineers. Depending on the operational condition, the traditional treatment of granular flow is to separate it into three different regimes, including a dense quasi-static, an intermediate and a gaseous regime (Forterre and Pouliquen 2008). Figure 1.1 depicts these three possible regimes of flow in an inclined plane geometry. Particles at the free surface form a dilute flow layer analogous to molecular gas (Forterre and Pouliquen 2008). In this state of flow, particles are assumed to interact

through binary collisions, and this mode of deformation can be referred to as the kinetic regime. The dissipative nature and the inelasticity of the particles will complicate this state of flow unless there is a constant supply of energy to the system, as in the granular flow on a vibrating screen. At the base of the flow in Figure 1.1, the flow is very slow and the dynamics are governed by inter-particle friction and enduring contacts (Roux and Combe 2003). This behaviour of granular material is described as the plastic solid flow or quasi-static regime (Holyoake 2012; Nedderman 2005). In the region between the kinetic and the quasi-static flow is a regime where granular materials flow like a liquid, and the particles interact both by collision and friction (MiDi 2004; Pouliquen and Chevoir 2002). The coexistence of the three flow regimes shown in Figure 1.1 can be described further as (i) quasi-static, (ii) dense (i.e. liquid-like which is kinematic), and (iii) inertial (turbulent). In practice, the distinction between these three regimes is complicated as they can exist simultaneously in granular flow.

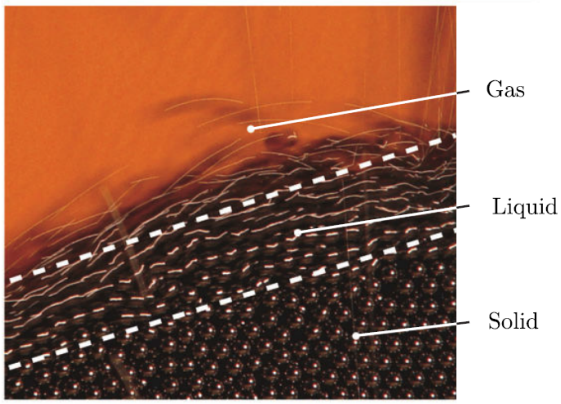

Figure 1.1: An illustration of the solid, liquid and gas flow regimes. Adapted from Forterre and Pouliquen (2008)

1.2 DEM modelling of granular flow on a vibrating screen

DEM has been used previously to study the design and optimization of industrial screening processes. Shimosaka et al. (2000) were the first to apply DEM to screening - they derived a phenomenological model of screening from a three-dimensional simulation on a batch-operated

screen with 400 particles. Subsequently, Li et al. (2002) and Li et al. (2003) investigated the influence of near-aperture size particles and the depth of the particle layer on screening efficiency in a continuous screen. Other studies, e.g Cleary (2004), Dong et al. (2009) and Alkhaldi and Eberhard (2007) have employed DEM to investigate several sub-processes of screening, on small-scale as well as large-scale screens. However, to the best knowledge of the author, none of this work studied screening from the perspective of granular rheology.

Other researchers have studied the rheology of granular flow of mono-size particles on inclined planes with rough surfaces. Silbert et al. (2001) performed a set of numerical simulations of granular media to investigate the rheology of cohensionless granular particles in inclined plane geometries (chute flow). Campbell (2002) identified different regimes in and the constitutive behaviour of granular flow using DEM simulations of the homogeneously sheared flow of cohensionless particles in the periodic domain. More recently, Vidyapati et al. (2012) showed by validating experimental data that DEM is capable of capturing the regime transition from the quasi-static to the intermediate regime. However, to the best knowledge of the author, none of this work has ever been extended to industrial vibrating, inclined screens separating particles with a distribution of sizes.

DEM uses the physics of particle interactions to provide information about the forces acting on individual particles and equipment surfaces (boundaries), and flow trajectories. It is a very useful tool that can provide detailed insight into screening processes and information about parameters that could be difficult to obtain empirically, such as solids concentration, shear rate, inter-particle friction coefficient, etc. (Vidyapati et al. 2012). The ability of DEM to probe micro-scale particle interactions makes it an ideal tool for studying the rheology of particle flow on a vibrating screen. Understanding the rheology of granular flow on a vibrating screen is the first step to developing a phenomenological model that will accurately predict the efficiency of industrial screens.

1.3 Hypothesis

DEM can be used to model the motion of particles through a vibrating screen, and can provide key information for testing and developing kinetic models of stress. A visco-plastic rheology based on frictional collisional stresses can be developed using DEM. A numerical (via DEM) characterization of granular flows in vibratory screens coupled with a model of the granular rheology of the system will provide mechanistic descriptions of the flow of granular matter along and through screens. The hypothesis is itemised as follows:

(i) DEM can generate data for the granular flow of particles on an inclined vibrating screen

(ii) A visco-plastic rheological model based on frictional collisional stresses can be developed to capture essential flow regimes observed on a vibrating screen

1.4 Objective and scope

It is the aim of this project, using DEM as a tool, to quantify the granular rheology of particles moving along a vibrating inclined plane, in order to be able to begin developing a phenomenological model of screening. This work focuses essentially on granular flow through a perforated plate, with application to screening of particulate materials. In this work a model of flow on an inclined vibrating screen will be developed that extends the visco-plastic rheology formation of Pouliquen et al. (2006) to capture the kinetic and turbulent stresses. The study will be restricted to dry particles, and will not consider soft particles, cohesive effects or the surrounding fluid.

The overall goal of this research is to develop a mechanistic model of screening which includes a description of the rheology of granular flow on a vibrating screen. This objective will be pursued by using the physics of particle interaction (DEM) to study the granular behaviour on a vibrating screen. Here, DEM will be used essentially to provide input to the models developed to study different transitional regimes of granular flow along the surface. The data

from DEM simulations will be employed to study the depth (h) of the particle bed, the solids concentration (ϕ) and the average velocity $\langle u \rangle$ of the granular avalanche along the screen.

In order to achieve the aforementioned objectives, DEM will be employed to simulate the motion of individual particles and to compute the contact forces between particles based on a contact mechanics model. The micro-scale information obtained from the simulation will give an insight to the collective behaviour of particles on the screen and guide the development of a continuum model to predict the granular rheology.

The following are the main objectives of this research:

(i) Employ DEM to generate data for the granular flow of particles on an inclined vibrating screen

(ii) Develop a visco-plastic granular rheological model to capture the essential flow regimes and their transitions on an inclined vibrating screen

Sub-objectives of this research are:

(i) Develop numerical solutions in relation to a vibrating screen surface to determine the average velocity, volume fraction (solids concentration), and the flow depth of particles on the screen.

(ii) Study the variation of the effective friction coefficient and the solids concentration with the inertial number, to determine all phases and capture the crucial phase transitions.

The thesis is organised as follows:

(i) Chapter 2 presents a review of screening and granular flow models.

(ii) Chapter 3 outlines the conditions for DEM simulations and the micro-macro transition method employed for data processing.

(iii) Chapter 4 develops a granular flow model with a particular focus on vibrating inclined screens.

(iv) Chapter 5 describes energy dissipation in the system, presents results and explains how the granular flow model developed in chapter 4 applies to screening.

(v) Chapter 6 presents the conclusions and recommendations.

Chapter 2

Literature Review

This review highlights the need for studying the rheology of granular flow on vibrating inclined screens and presents previous research on the rheological behavior of granular matter. It further discusses different screening models including Discrete Element Methods (DEM) models and relevant parameters / variables for modelling granular flow on vibrating screens. In addition, the chapter discusses granular flow modelling of vibrating screens, measurements in inclined planes and the kinematics of granular flow down an incline plane. The effects of vibration on granular mixtures, segregation and screening, DEM contact model and DEM application to screening are discussed as well.

2.1 Vibrating screens

Sieving is an old practice of physical separation dating back thousands of years (Makinde et al. 2015; Li et al. 2015). Vibrating screens such as the one depicted in Figure 2.1 are used extensively in mineral processing to perform size classification. Common to all vibrating screens is a screening surface consisting of apertures through which granular materials are screened. Depending on the separation size, vibrating screens often have multiple decks, and large screens can process several thousand tonnes per hour. The vibrating motion of the screening surface and the inclination of the surface (in the case of vibrating inclined screens)

help to position particles at different orientations as they travel down the slope. The undersize particles have several opportunities to fall through the apertures while oversize particles flow down along the screening surface. In practice, some undersize particles escape to the oversize collector, reducing the efficiency of the separation (Cleary 2004).

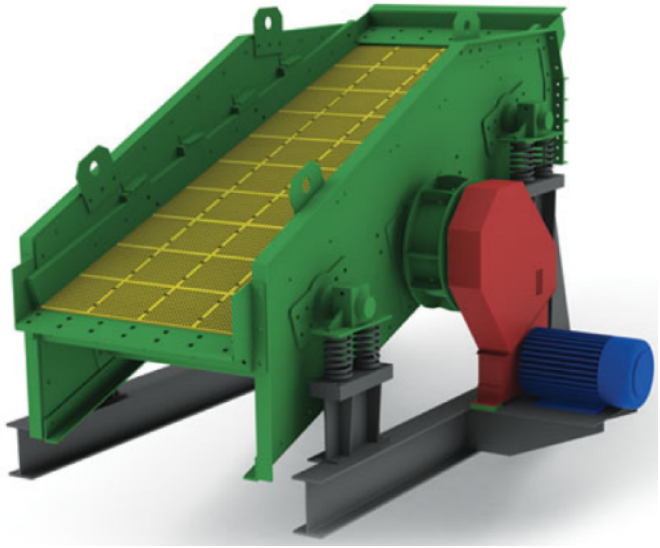

Figure 2.1: Vibrating inclined screen

Typically, a mixture of fine and coarse particles is fed to the screen at one end and is transported by the vibrating motion of the screen to the other end, where oversize material is collected, as illustrated in Figure 2.2. The undersize material ideally should fall through the apertures of the screen, but the probability of this depends on how it is presented to the screen. The basic process along the screen is divided into the following steps:

(i) Stratification (migration of undersize particles to the screen surface due to the vibration condition)

(ii) Passage of fine particles through the apertures

(iii) Transport of the oversize material over the screen surface to the oversize collector, and the undersize through the screen surface to the undersize collector (Meinel 1998)

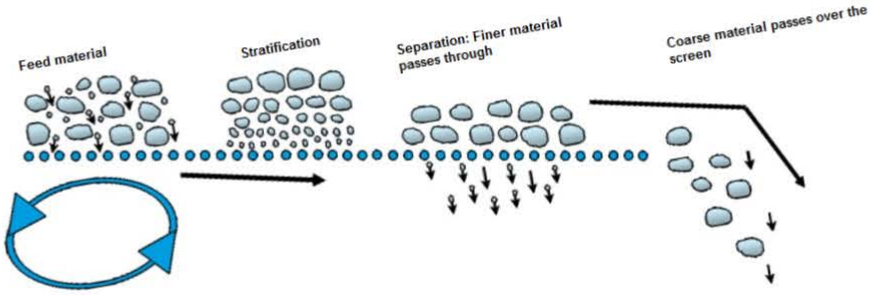

Figure 2.2: Stratification of particles on a screen

2.1.1 Screening variables

There are many factors contributing to the performance of industrial screens and, currently, not all of these are incorporated into available screening models. Parameters that affect screening performance range from the nature of the feed material and how it is being presented to the screen and the motion of the screen and the interaction of the materials on the screen. Figure 2.3 shows the different variables that affect screening efficiency at different stages of screening using vibrating screens. All the parameters listed in Figure 2.3 are very essential, especially in numerical (DEM) modelling. Much work has been reported in the literature on the effects of these factors on screening performance (Hilden 2007; Leonard and Hardinge 1991; Tsakalakis 2001; Yanhua and Xin 2010; Li et al. 2002). However, the information in most studies is mostly qualitative and related to specific screen designs and feed materials. Some general information exists but with contradictory data (Hilden 2007).

One of the most important parameters affecting the performance of vibrating screens is the vibration intensity, which combines vibration stroke and frequency. This parameter is a key factor affecting the speed of the bed along the screen and the residence time on the screen. It enables stratification of the bed and controls the extent to which near size particles blind and peg the screen aperture (Hilden 2007).

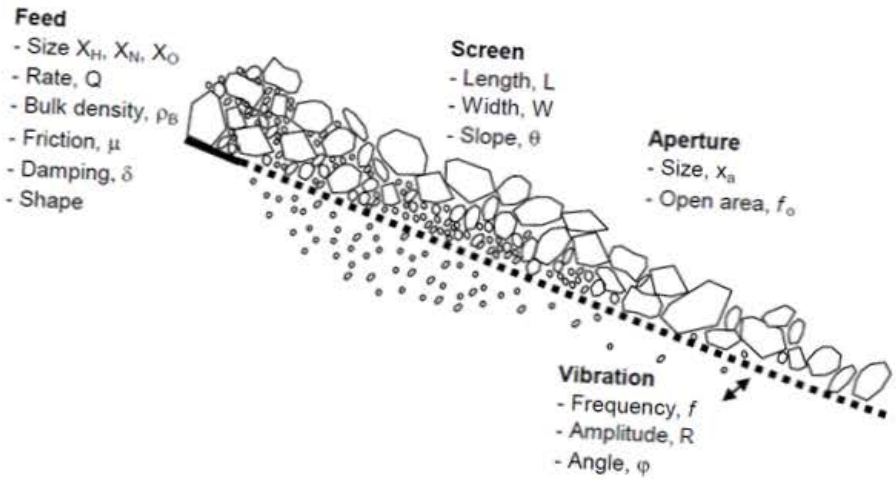

Figure 2.3: Screening variables

The speed of the bed movement is another important factor in determining screen performance. According to Soldinger (2002), the bed velocity determines the bed thickness at a given feed rate, and the capacity of the screening process. In order to study the movement of the bed along the screen, both theoretical and empirical models have been developed to estimate the transport velocity on screens (Soldinger 2002; Tsakalakis 2001). These models incorporate screen slope, material characteristics, screening surface parameters and vibration characteristics. However, little or no work has been done on the rheology of granular flow on screen surfaces and on the different flow regimes that can be observed during screening. Understanding the rheology of granular flow on the screen will help characterise the flow, identify the dominant stresses, and the energy dissipation in the flow. This thesis postulates that the rheology of granular flow is key to understanding the particle behavior along a dynamic vibrating screen, and to predicting screen performance.

2.1.2 Granular mixtures, segregation and screening

In nature, and in industrial applications, granular materials are often poly-dispersed, and comprised of particles of varying characteristics, such as shape, size, density and other possible physical properties (Tunuguntla 2015). When multi-component granular flow is subjected

to external forces, like shear and vibration, the flow exhibits a variety of phenomena, e.g. segregation and percolation (Fan et al. 2014), which are essential to screening. In this study, for the purpose of modelling, we classify granular flow on a vibrating screen as a *binary flow* (undersize and oversize particles) over a separating medium. Two processes occur simultaneously during screening, i.e. stratification (segregation) and passage of particles through the apertures in the screen surface. Segregation, as an important phenomenon in binary granular flow (Fan et al. 2014; Rosato et al. 2002; Van der Vaart et al. 2015; Tripathi and Khakhar 2011), is known to cause many problems in the handling of bulk solids as well as in geophysical flows (Rosato et al. 2002). It is a process where a homogenous bulk of granules composed of different constituents becomes spatially non-uniform as a result of the relative motion within the materials.

To enhance the passage of particles through the apertures in the screen surface, particles must stratify, and this stratification is achieved by subjecting the granular flow to vibration. According to Hilden (2007), Williams (1963) performed the first qualitative studies on the effect of vibration frequency on the motion of a single large sphere in a bed of sand oscillated vertically. He attributed the upward movement of the large sphere to the locking effect of smaller particles which move beneath the large particle during vibration. In a further analysis, Williams (1976) highlighted the properties that promote segregation, including particle size, shape, density and elasticity. He also described three mechanisms of segregation, viz the trajectory of segregation, the percolation of fine particles and the rise of coarse particles during vibration.

The segregation process has been modelled empirically by some authors (Ciamarra et al. 2006; De Silva et al. 2000; Olsen and Rippie 1964; Faiman and Rippie 1965) using first-order kinetics to develop an equilibrium state characterized by a balance between mixing and separation. Hsiau and Wang (1999) employed image technology (CCD image sensor) in an experiment to determine the influence of the vibrational acceleration amplitude on a binary mixture in

a vertical bed. They observed that the absolute segregation rate and the velocities of both sizes decreased with time until they finally become zero. Rosato et al. (1987) employed the Monte-Carlo simulation technique to show that a local geometrical void-filling mechanism can lead to size segregation (called the Brazil nut effect). Jha and Puri (2009) studied percolation segregation under a periodic movement, and derived a relationship between the intensity of vibration, the normalised segregation and the strain rate of particles

Segregation is essentially caused by the physical properties of particulate materials and can also be induced as in the case of vibrating screens. As may be seen in Figure 2.3, the percolation of fine materials is essential for screening; this implies that similar factors affect screening and segregation. These factors include the size and shape of particles relative to the apertures of the screen, the mesh size of the sieve, the depth of flow of the particles on the screen, the direction of flow, and the flow rate of the material relative to the movement of the screen surface (El Khatib 2013; Allen 2013; Hilden 2007). A review of different factors affecting screening has been carried out by Hilden (2007).

The rheology of granular matter describes its flow and the transition in the flow. Granular matter can exhibit constitutive behaviour like a solid, liquid, or gas depending on the level of agitation. The different constitutive behaviour depends on microscale properties (like particle friction and coefficient of restitution) as well as macroscale properties (like shear rate and solids concentration) (Vidyapati and Subramaniam 2012). The rheology is governed by a local friction law that relates the effective friction coefficient, μ, and a single dimensionless variable parameter, the inertial number, I which signifies the dynamic effects of the flow. Tripathi and Khakhar (2011) studied the rheological properties of a binary mixture in dense regime flow. They analysed the effect of rheological properties such as solids concentration, depth of particle flow, shear stress and the effective friction on the segregation process. Among other things, they observed that the mean velocity of both components is the same for all the mixtures and that there is no slip velocity between the components. Further, they noted that

granular mixtures follow a linear dilatancy law, as in the case of mono-disperse particles. In the binary mixture, they observed that the viscosity varies with depth of flow, and depends on bulk density, size ratio, and the degree of segregation. Finally they have proposed a modified mixture rheological model for a well-mixed and granular mixtures differing in size and density.

Due to the complexity of the interactions between variables during screening, no satisfactory method of predicting the throughput of industrial screens has yet been developed (Sultanbawa et al. 2001). Among other factors, the inability to predict the throughput of industrial screens as well as confusing laboratory sieve analysis have led to the inefficient operation of industrial screens (El Khatib 2013). Most studies on screening (Tsai and Chang 2009; Liu 2009; Moon et al. 2008; Chen and Xin 2009) focus on the effect of various operational parameters and screening methods on the screening efficiency or on the analysis of screening kinetics (Wodzinski 2003; Shaviv 2004).

2.1.3 Effects of vibration

Vibration is a form of external energy supplied to fluidize a granular system. Due to the dissipative nature of a granular system, this energy must be added in order to sustain the system in a steady state. A model relating the energy input by a vibrating wall to the energy dissipation in collisions was developed by Warr et al. (1995). They investigated the fluidization behaviour of a two-dimensional granular material under a vertical vibration, and measured the solids concentration and the velocity distribution function. Under vibration, dry granular material undergoes a variety of phenomena which include fluidization (Clement and Rajchenbach 1991; Ford et al. 2008; D'anna et al. 2003), segregation (Ahmad and Smalley 1973; Huerta and Ruiz-Suárez 2004; Rosato et al. 2002), undulation (Douady et al. 1989; Clément et al. 1996; Sano 2005), the granular Leidenfrost effect (Eshuis et al. 2005), and the formation of wave patterns reminiscent of the Faraday waves in a liquid (Melo et al. 1994; Moon et al. 2001; Faraday 1831; Cross and Hohenberg 1993).

The stroke and frequency of vibration are essential factors that affect the speed of a bed along a screen, and consequently the residence time on the screen (Hilden 2007). Further, because the stroke enables stratification of the bed, it controls the extent to which particles peg or blind the screen aperture. Clearly, vibration should be optimised to prevent mixing and the ejection of particles from the apertures while they attempt to pass through, while providing repeated chances for particle passage.

2.2 Kinematics of granular flow down inclined planes

As discussed in Chapter 1, modelling granular flows on inclined planes still poses some challenging problems. Depending on the nature of the flow regime, granular flow can be frictional, collisional or intermediate (see Figure 1.1). In a dilute and highly sheared medium, the particles interact via collision and a constitutive law similar to the kinetic theory for dense gases can be deduced. In the case of a dense granular medium, the particles are sheared slowly and are in constant contact. They dissipate energy by friction and the constitutive law is plastic-like (Berton et al. 2003).

In inclined chute flow, no distinct flow regime can be attributed to the nature of the flow in the system due to the anomalous behaviour of the flow, and both particle friction and collision play important roles. A lot of work has been reported in the literature with regards to the flow on an inclined chute, but no constitutive law has been proposed to capture the various regimes of flow. Researchers have investigated the transition between solid, liquid and kinetic regimes using numerical simulation and theoretical models of disks in plane shear (MiDi 2004; Lois et al. 2006; Da Cruz et al. 2003; Roux and Radjai 1998).

A pile of sand on an inclined plane assumes a solid-like position until it is inclined above a critical angle. At the onset of flow, the tangent of the slope of the pile, which is the ratio of the shear stress to the normal stress, has to reach a critical value called the friction coefficient

in order for the material to deform (Daerr and Douady 1999).

Scientists have attempted to model the deformation that occurs in the transition from solid to liquid granular regimes by proposing a plastic constitutive law (MiDi 2004; Roux and Radjai 1998; Daerr and Douady 1999) and trying to relate the microstructure to the macroscopic behaviour (Roux 2002). However, this model does not predict continuous quasi-static granular flow; it only focuses on the initiation of the deformation. Further, it cannot describe the hysteresis observed in a stress-driven system. For instance, granular materials on an inclined plane will only start flowing when the angle of inclination is above the critical value and will stop flowing below this angle. This analysis shows that a balance of energy input and energy dissipation is relevant to granular hysteresis (Forterre and Pouliquen 2008).

In addition to the solid-to-liquid transition, when granular media is strongly agitated as in the case of a vibrating screen, the granular medium becomes dilute and behaves like a gas. Many researchers have developed a kinetic theory of granular gases (Goldhirsch 2003; Forterre and Pouliquen 2002; Swinney and Rericha 2004; Da Cruz et al. 2003; Lois et al. 2006) for this regime. Particles in this regime interact by binary collision analogous to classical gases but there is a difference in that kinetic energy is lost during collisions. Collisions are characterized by the restitution coefficient (e) which is the measure of the ratio between the velocities of the particles before and after collision.

The kinetic approach provides a set of constitutive equations which combines the average density, the mean velocity and the fluctuation velocity, (which is a function of the granular temperature). Some authors have investigated the transition between the liquid and kinetic regimes using numerical simulation of disks in plane shear (Da Cruz et al. 2003; Lois et al. 2006). According to Forterre and Pouliquen (2008), most researchers agree that the coefficient of restitution, (e), is essential to the transition from the liquid to the kinetic regime. As shown in Figure 2.4, the range of the volume fraction in the liquid regime increases when the

coefficient of restitution decreases. Beyond the critical volume fraction, the uniform liquid regime becomes deformed and a transition occurs.

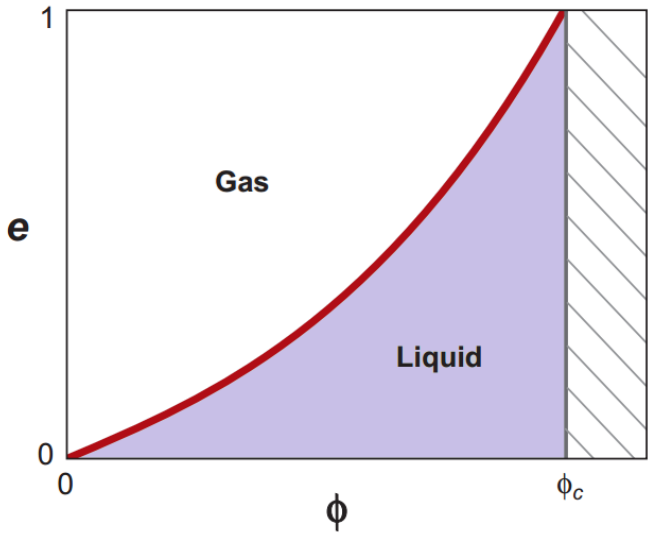

Figure 2.4: Phase diagram for volume fraction and the coefficient of restitution. Adapted from Forterre and Pouliquen (2008)

2.3 Measurements in inclined planes

Work has been done on various techniques to measure the different flow properties of granular material down rough inclined planes ((Pouliquen 1999a; Azanza et al. 1999; Ancey 2002; MiDi 2004); and references therein). Most measurements are taken in steady state flow along a line similar to the y-axis in Figure 2.5. The principal observations from these measurements reveal a constant volume fraction across the layer, and that the Bagnold scaling of velocity varies with depth to the power of 3/2 for thick layers of flow and almost linearly for a thin flow (Rajchenbach 2003; Silbert et al. 2003; Forterre and Pouliquen 2008).

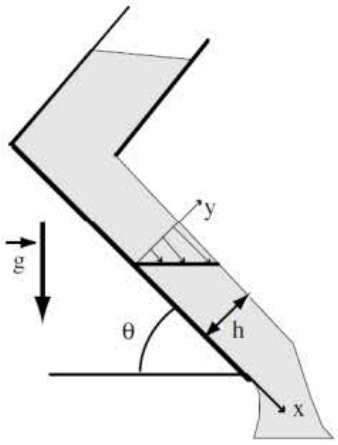

Figure 2.5: Granular flow down a rough inclined plane. Adapted from MiDi (2004)

2.4 Granular flow modelling of vibrating screens

A comprehensive review of screening models and approaches to screen modelling can be found in Hilden (2007). The approaches include the empirical or factor method (Kelly and Spottiswood 1982; King 2001), the use of efficiency curves (mathematical models) which include probability and kinetic models (Hilden 2007; Dehghani et al. 2002; Abdel-Aziz 1971; Whiten and White 1979; Grozubinsky et al. 1998; Kaye and Robb 1979), physical models using dimensional analysis (Hilden 2007), and discrete element method (DEM) modelling (Cleary and Sawley 2002; Yanhua and Xin 2010; Chen and Xin 2009; Djordjevic 2003a;b).

Factor models have been developed by screen manufacturers to enable screen users to estimate screening area requirements. These models express screening capacity in tonnes per screen area as a function of aperture size. Adjustments are made for various factors related to the screen design and material properties. According to Hilden (2007), the methods used to derive these factors are not available in published literature but they are derived from large data-bases of screening data which are confidential to the manufacturers of screening machines. There are different versions of these models with various factors, and efforts to develop a standard empirical model have not been successful.

Extensions to the standard empirical factor models by Karra (1979) are considered to be specific to the system he studied, and do not apply to all screening applications (Hess 1983). Although these models are easy to apply, and are popular especially with aggregate producers, interactions between variables are assumed not to exist and little insight is given into the mechanics of the process (Roberto 1992). It is therefore recommended that factor models be used as a guide to estimating screening requirements (Hilden 2007)).

While the factor method to modelling screening is still relevant in industrial practice, especially in the aggregate industry, much work has been done on semi-empirical or mathematical modelling of screens, usually based on a probability or kinetic hypothesis. The following are some available screen models in the literature: Gaudin et al. (1939); Shigeo (1960); Whiten and Herbst (1984); Whiten and White (1979); Hilden (2007); Batterham et al. (1980); Ferrara and Preti (1975); Ferrara et al. (1988); Subasinghe et al. (1990; 1989); Soldinger (1999; 2000; 2002).

The Gaudin formula is expressed as:

$$P(x) = \left[\frac{x_a - x}{x_a + x_w}\right]^2. \tag{2.1}$$

This is a probability model, where $P(x)$ is the probability that a spherical particle of diameter x will pass through a square aperture (x_a) of size x_w. The probability that a particle will not pass through the screen in n times is given as:

$$P'(x) = (1 - P(x))^n \tag{2.2}$$

Other probability approaches are mostly modifications of Gaudin's model, e.g Miwa (1960):

$$E(x) = exp\left[-n_L L \frac{(x_a - x)^2}{x_a^2}\right] \tag{2.3}$$

where $E(x)$ is the same as $P(x)$, n_L refers to the number of attempts of passage per unit length, L is the length of the screen, and x_a is the aperture size.

Whiten (Hilden 2007) developed a similar model:

$$E(x) = exp\left[n_t\left(\frac{x_a - x}{x_a - x_w}\right)^2\right] \tag{2.4}$$

As in Miwa's model, n_t is a fitted parameter that corresponds to the number of attempts, x_w is the diameter of the wire, and x_a is the screen aperture.

Batterham et al. (1980) developed a probability model (different from the Gaudin's model) from the empirical efficiency curve model of Mular and Bhappu (1978):

$$E(x) = \frac{1}{1 + exp\left[\frac{x_{50}^3 - x^3}{k}\right]} \tag{2.5}$$

This model, according to Dehghani et al. (2002), is more accurate than models developed from Gaudin's expression. The parameter x_{50} is the cut-size (where screen efficiency is 0.5), which Batterham's results describe as a function of screen aperture.

Ferrara and Preti (1975) and Ferrara et al. (1988) developed a kinetic model for the rate of screening. Passage is assumed to be zero order process when the screen is crowded and a first order process when the bed depth is small. The model does not consider stratification because the materials on the screen are assumed to be perfectly mixed. The zero-order kinetic equation for crowded conditions is given as:

$$E(x) = exp\left[-k_i \int_0^L \frac{dL}{F}\right] \tag{2.6}$$

while for the low depth, the first order equation is:

$$E(x) = exp(-s_i L) \tag{2.7}$$

where L is the length of the screen, F is the rate of flow of particles per unit width on the screen, and k_i and s_i are the kinetic constants for each size interval. Subasinghe et al. (1990) and Soldinger (1999; 2000; 2002) derived a screen performance model using first-order kinetic parameters from a range of empirical data. Their model describes both passage and stratification as simultaneous and interrelated processes. Soldinger (2002) incorporated a velocity transport model that relates the the bed velocity to the vibration characteristics and the screen slope. This model is very useful, but it requires kinetic experimental data from the actual industrial screen being modelled, for fitting purposes.

2.5 Discrete Element Method (DEM) modelling

Initially pioneered by Cundall and Strack (1979) to study soil mechanics, DEM has since been adapted to study systems such as vibrating screens, tumbling mills and other mineral processing systems. The macroscopic behaviour of particulate flow can be determined by the microscopic interactions between particles and between particles and a boundary. It is a very useful tool that can provide detailed insight into screening processes such as the frequency of collision, the average velocity of flow, and the duration of inter-particle contacts, as well as information on the collective flow of granular materials on a screen. A typical visualization of DEM application in screening is given in Figure 2.6

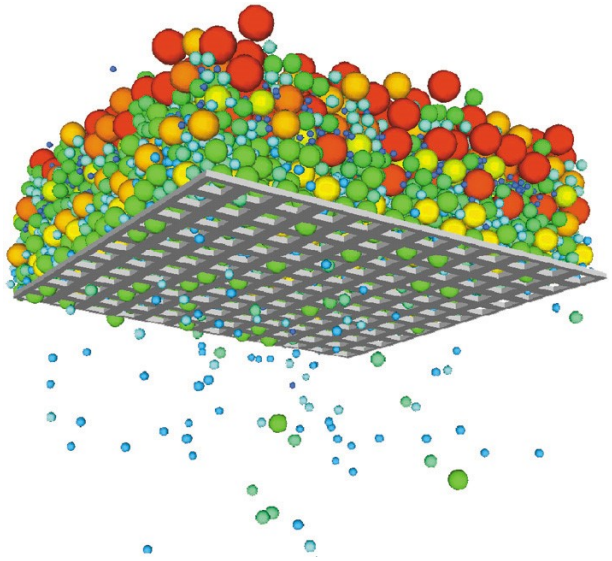

Figure 2.6: DEM visualization of screening

DEM gives insights into parameters that are difficult to obtain empirically, such as solids concentration, shear rate, inter-particle friction coefficient, etc. (Vidyapati et al. 2012). Shimosaka et al. (2000) were the first to apply DEM to screening - they derived a phenomenological model of screening from a three-dimensional simulation on a batch-operated screen with 400 particles. Li et al. (2002; 2003) investigated the influence of near-aperture-size particles and the depth of the particle layer on screening efficiency in a continuous screen. Other studies (e.g. Cleary (2004); Dong et al. (2009); Alkhaldi and Eberhard (2007); Chen et al. (2010)) have used DEM to investigate several sub-processes of screening, on small-scale as well as large-scale screens.

Generally, granular systems are composed of discrete particles which can be described by Newton's laws of motion. For instance, the translational motion of particle i under the influence of gravity, g, and the resultant force for every particle i in a system is described as follows:

$$\nu_i = \frac{dx_i}{dt} \tag{2.8}$$

$$m_i \frac{d\nu_i}{dt} = \sum_{j=1}^{n_i} (F_{c,ij} + F_{d,ij}) + m_i g + F_i \tag{2.9}$$

$$\frac{d\omega_i}{dt} = \frac{1}{2L_i} \sum_{j=1}^{n_i} x_{ij} \times F_{c,ij} \tag{2.10}$$

where m_i, ν_i and x_i are the mass, velocity and position of the particle at time t, and n is the number of particles in contact with particle i. The total force on the particle can be calculated as the sum of four likely forces that could act on the particle. These forces are the contact force, F_c; the damping force, F_d; the gravity force, g; and force F_i, which is calculated in the event of other forces like drag, magnetic field or cohesion acting on the particle. Equation 2.10 is used to determine the rotational force on each particle where L_i is the moment of inertia and ω_i is the rotational velocity of the particle.

2.5.1 Contact model

The contact model describes the interactions and behaviour of particles when in contact with each other and the system geometry. Interaction models are chosen to accurately represent the physical system. The common contact-model approaches used for DEM simulation are: linear spring and dashpot; Walton and Braun (Walton and Braun 1986) and Hertz-Mindlin (Hertz 1886) contact model. Although many contact models have been used in the literature for DEM simulations, the majority are slight variations of these three approaches (Bbosa 2013; Zhu et al. 2007).

Generally, the most intuitive models used are the linear models, the most common of which is the spring and dashpot model proposed by Cundall and Strack (1979). In this model, shown in Figure 2.7, the spring explains the elastic deformation during collision, while the dashpot describes the viscous dissipation. This model has been widely used in DEM analysis of granular flow and in screening (Tsuji et al. 1993; Govender et al. 2004; Li et al. 2002; 2003;

Cleary 2004). Equations 2.11 and 2.12 show the two components of the contact force between colliding particles in a spring and dashpot model:

$$F_n = -k\psi_n - \varsigma\nu_n \tag{2.11}$$

$$F_t = -k\psi_t - \varsigma\nu_t \tag{2.12}$$

where ψ_n and ψ_t are particle displacement in the normal and tangential directions, while ν_n and ν_t are the corresponding relative velocities; K is the spring stiffness of a material; and ς is the viscous dissipation or the damping force (Li et al. 2003). As depicted in Figure 2.7, particles slide over each other when the tangential force, F_t, exceeds the limiting frictional force: the tangential force is calculated using the frictional coefficient, f, i.e.

$$F_t = -fF_n \tag{2.13}$$

However, according to Mohr-Coulomb's law, the shear force cannot exceed the product of the frictional coefficient and the frictional force. While the spring and dashpot model represents the contact force by a linear spring damping element, Hunt and Crossley (1975) argued that a linear damping model does not truly reflect the physical nature of the energy transfer process, i.e. the contact force is discontinuous because of the damping term. They proposed a non-linear damping force model based on Hertz (1886) theory of contact (Gilardi and Sharf 2002).

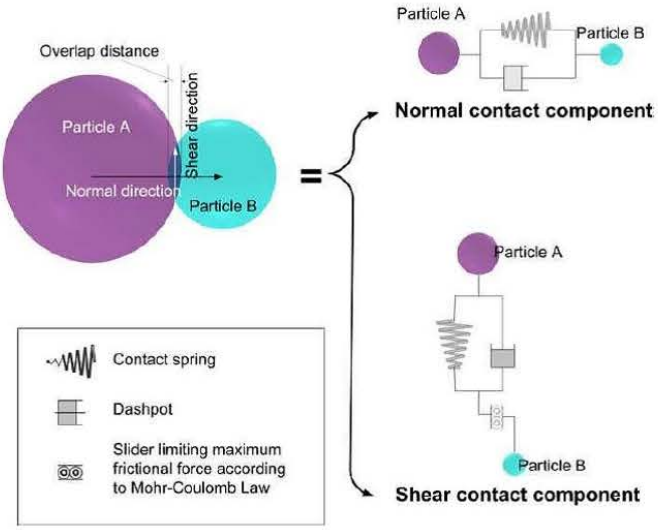

Figure 2.7: Schematic of the approach used with the linear spring and dashpot contact model. Adapted by the author from Govender et al. (2004)

The spring and dashpot model depicted in Figure 2.7 describes the interaction of particles when they come into contact with each other or with the physical geometry defined in DEM simulation. Here, the contact forces between two particles A and B are decomposed into normal F_n and tangential F_t components. The impact of these forces and the resulting motion of the particles at different time steps are numerically integrated for all the particles in the system in three dimensions, and exported as a text file for further analysis using a mathematical tool like MATLAB.

The application of Hertz-Mindlin model to DEM was proposed by Di Renzo and Di Maio (2004; 2005) and Peng (2014). This contact model has also been used in the DEM simulation of screening processes to provide an accurate representation of the screening collision environment (Chen and Xin 2009; Li et al. 2002; Xiao and Tong 2012). Other screening models are discussed by Kruggel-Emden and Elskamp (2014), who published a detailed review of different phenomenological models available for the design and optimization of the operating parameters of screening. These models address different complexities that provide information on the screening rate or efficiency, but not from a rheological perspective.

2.6 Granular rheology

While the models described in Section 2.4 essentially capture the qualitative features of vibrating screen efficiency, the absence of a clear rheological description has limited their value. Fortunately, progress has been made towards a constitutive law for dense granular flow in the last decade (Pathmathas 2015). MiDi (2004) observed from different flow geometries that the relevant parameters for the flow of cohesionless rigid spheres in which boundary effects are negligible are the shear rate, $\dot{\gamma}$, pressure P, and bulk density, ρ, expressed as:

$$\rho = \phi\rho_p \tag{2.14}$$

where ϕ is the solids concentration (volume fraction) and ρ_p represents the particle density of the spheres. From dimensional analysis of numerical data, Da Cruz et al. (2005) and Iordanoff and Khonsari (2004) claimed that the only significant dimensionless control parameter is the *Inertial number* (I):

$$I = \frac{|\dot{\gamma}|d}{\sqrt{P/\rho_p}} \tag{2.15}$$

which singly controls the flow. $|\dot{\gamma}|$ is the norm of the shear rate and P is the confining pressure. Physically, the inertial number I represents the ratio between the microscopic (rearrangement) time scale $\frac{d}{\sqrt{P/\rho_p}}$ (where d is the diameter of the particle) and the macroscopic (deformation) time scale $1/\dot{\gamma}$. It (I) describes the relative importance of inertia and confining stresses. A schematic representation of the physical meaning of the two time scales is shown in Figure 2.8. For a layer of shearing particles (grains), T_γ is the macroscopic time needed for one layer to move a distance d over the layer below it. T_p corresponds to the time needed for the top layer to push back to its original position after having to climb over the next particle.

From the description of I, in equation 2.15, we can characterise the type of flow in a granular system. For instance, in a slow (quasi-static) flow, I has a small value because the movement between layers of particles is slow, and particles' inertia has little effect. Conversely, in dilute or agitated flows with large shear rates, the particles' inertia overcomes the confinement force in the system, and, hence, the value of I is large (Holyoake 2012).

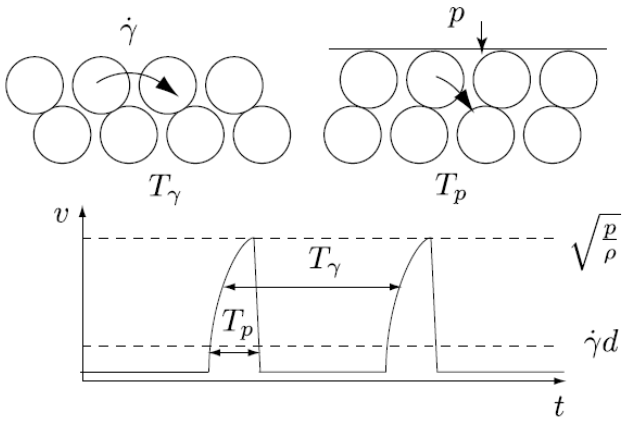

Figure 2.8: Schematic representation of the physical meaning of the microscopic time scale T_p and macroscopic time scale $T_{\dot{\gamma}}$. Reproduced from MiDi (2004)

An important consequence is that the solids concentration (ϕ) and the dimensionless stress (τ) must be functions of the inertial number (I) such that the resulting granular flow is given by an effective friction coefficient (μ), i.e.

$$\phi = \phi(I) \tag{2.16}$$

and

$$|\tau| = \mu(I) \tag{2.17}$$

Within a homogenous state, the volume concentration (ϕ) and effective friction coefficient

(μ), vary linearly with the initial number I as:

$$\phi(I) = \phi_{max} - aI, \tag{2.18}$$

$$\mu(I) = \mu_{min} + bI \tag{2.19}$$

where ϕ_{max}, ϕ_{min}, a, and b are constants (Savage 1984; Ancey et al. 1999; Pathmathas 2015).

Consistent with the dimensional analysis of Da Cruz et al. (2005), the solids concentration ϕ and dimensional stress $\mu = |\frac{\tau}{P}|$ should be slaved to the inertial number I such that the resulting granular flow is determined by $\mu(I)$ and $\phi(I)$. By assuming that this essential local rheology applies throughout the bed, Jop et al. (2005) showed compatibility between the constitutive equations for granular flow and their experimentally determined basal friction (resistance to the flow on the surface) law by choosing the effective friction coefficient of the form:

$$\mu(I) = \mu_{min} + \frac{\mu_{max} - \mu_{min}}{I/I_0 + 1} \tag{2.20}$$

where $I_o = 0.279$ is a constant determined by Jop et al. (2005) and μ_{min} and μ_{max} are respectively the friction coefficients that bound the steady flow. The corresponding expression for $\phi(I)$ was a linear function fitted as:

$$\phi(I) = \phi_{max} + (\phi_{min} - \phi_{max})I \tag{2.21}$$

with typical values taken as $\phi_{max} = 0.6$ and $\phi_{min} = 0.4$ (Pouliquen et al. 2006; MiDi 2004). Taken together, equations 2.16 to 2.21 are the constitutive laws for characterising dense granular flow.

In the case of granular flow on a vibrating screen, a dense flow and a liquid-like regime are

observed in the bulk of the flow, while the region close to the surface behaves more like a gaseous regime. However, the roughness of the surface of the screen created by the apertures causes resistance to the flow along the screen. This resistance is similar to the basal friction in equation 2.20. The choice by Jop et al. (2006) to extend the local rheology description to the entire bed is based on the measurements obtained by MiDi (2004) who suggested that the volume fraction ϕ, which remained nearly constant across the flowing layer, should be a function of the inertial number I. Based on this premise, the effective friction coefficient proposed by Jop et al. (2005) allows for the successful characterisation of the granular rheology across a wide range of granular flow configurations.

An interesting phenomenon is the transitions that must exist between the three flow regimes, and the hysteresis between the solid and the liquid layer, which this essentially empirical rheology does not capture. Lee and Huang (2012) employed rate-independent and rate-dependent components for the static and kinetic contributions of the shear stress, respectively, to address these limitations. The granular kinetic theory proposed by Jenkins and Savage (1983) was used for the kinetic contribution while the static contribution conformed to the friction law of Jop et al. (2006) and the dilatancy law of Hatano (2007).

Lee and Huang (2012) observed that there exists a kinetic stress in the flow, which results from the transition from liquid-like to gas-like flow (Figure 2.8). The first turning point in Figure 2.8 is the hysteresis at flow initiation while the second turning point is the transition from liquid-like flow to gas-like flow. Lee and Huang (2012) acknowledged that the discontinuity at the transition to the inertial flow regime (second turning point) warranted further study.

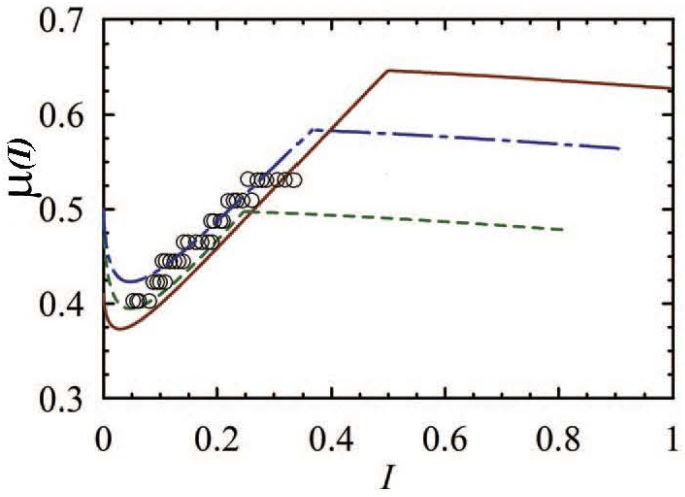

Figure 2.9: Variation of the effective friction coefficient with inertial number. The lines are model predictions for three different effective restitution coefficients while the open circles correspond to the data from MiDi (2004). Adapted by the author from Lee and Huang (2012)

2.7 Summary

Although simple in concept, the modelling of screen performance for better efficiency is not trivial. A review of the different factors influencing the performance of industrial screens has been presented above. Previous researchers have employed different modelling methods ranging from empirical to numerical and mathematical analysis to tackle screening problems. Although these have had varying degrees of success, much work still needs to be done in order to accurately predict the efficiency of industrial screens.

To go beyond the current state-of-the-art in screen modelling, a clear understanding of the particle motion along an inclined vibrating screen is required. To this end, the present work takes the step in the study of the rheological behaviour of granular materials on vibrating inclined screens. This work acknowledges that much has already been done to improve screening efficiency but, to the best knowledge of the author, little or no work has been done from a rheological perspective.

Generally, granular systems exhibit unique rheology that is not akin to fluids - i.e neither Newtonian nor non-Newtonian. This unique rheology makes the study of granular behaviour difficult, as particles exhibit a range of complex phenomena such as mixing, segregation and percolation. (These phenomena occur during screening and different parameters are varied in order to influence or inhibit them to achieve maximal efficiency. For instance, while mixing is not important in screening, segregation and percolation are essential for effective screening performance.) In order to study this unique rheology, efforts have been made to quantify granular rheology in different media with the aim of developing a universally accepted model for granular rheology. MiDi (2004) compiled the list of these studies and more efforts are being made towards developing this model.

This review has identified key elements relevant to quantifying granular rheology on vibrating screen, including the depth of the particle bed along the screen, the solids concentration, and the average velocity of the granular avalanche on the screen. Further, it was established from previous relevant studies that granular flow exhibits three different flow regimes: a dense quasi-static regime, in which particles are very slow and interact by frictional contacts; an intermediate liquid regime, in which the material is dense but still flows like a liquid with the particles interacting both by collision and friction; and a gaseous regime, in which the flow is very rapid, dilute, and the particle interact by collision.

To begin developing a phenomenological model for granular flow on an inclined vibrating screen, there is a need to develop a constitutive stress model that will capture all the stresses in the flow that cause different flow regimes, and the transition between one regime and another. The different constitutive behaviours depend on microscale properties (such as particle friction and coefficient of restitution) as well as macroscale properties (like shear rate and solids concentration). The rheology is governed by a local friction law that relates the effective friction coefficient, μ, to a single dimensionless variable parameter, the inertial number, I. Among all methods of screening modelling discussed in this review, DEM is

considered most appropriate for this study because of its ability to simulate by combining both the microscale and the macroscale properties of screening needed for this work.

Chapter 3

Modelling and Data Analysis

The numerical program and the analysis schemes undertaken in this thesis are reported in this chapter. Continuum models need to be calibrated and validated with available discrete empirical or numerical data. To achieve this, an efficient micro-macro transition method is required to obtain continuum fields such as momentum, density, stress, pressure, etc., from discrete individual particle data such as position, orientation, velocity, forces on individual particles, etc. This chapter presents the approach that was employed to address the objectives set out in the introduction. The continuum models formulated in this work were validated using numerical data from computational simulations.

3.1 Numerical modelling

To simulate a screening process, the key boundary is a woven mesh which provides apertures for undersize particles to fall through. To ensure better performance, additional parameters such as mechanical vibration and screen inclination are also employed. The 3-D DEM model shown in Figure 3.1 was set up to simulate granular flow on an inclined vibrating screen. The screen geometry was designed using computer aided design (CAD) in solidworks software and imported into the commercial package EDEM, developed by DEM solutions. EDEM is based on the Cundall and Strack (1979) algorithm and the appropriate contact model DEM-

Solutions (2006).

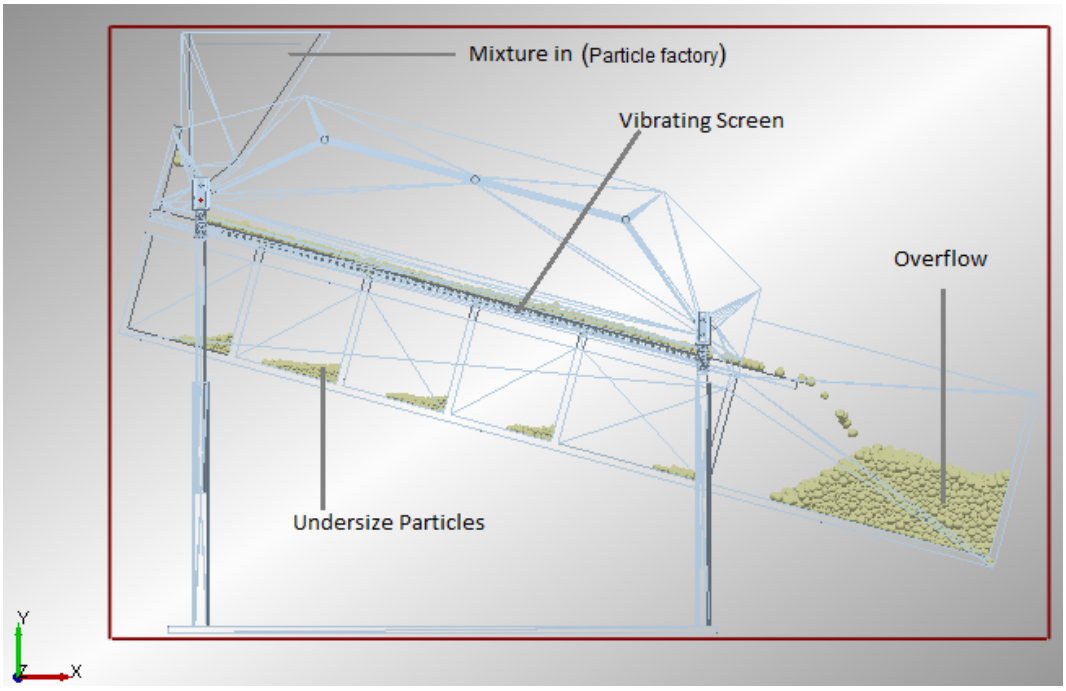

Figure 3.1: Schematic layout of the screening model

Simulations were conducted to model the separation of a mixture of dry, spherical, glass beads consisting of an equal volume of two differently sized particles. The modelling conditions employed in the simulations are listed in Table 3.1. The screen was 450 mm long and 308 mm wide, with square apertures of 3.5 mm. Simulations were performed using the conditions on Table 3.1 in order to build a data base from which the rheology of flow could be characterised. The selection of the screen vibration is based on the analysis of Chen and Xin (2009).

In each simulation, the binary mixture of particles was fed onto the screen by gravity, via the particle factory (feed hopper). At the moment of generation, the velocity was assumed to be $v_x = v_z = 0$ and $v_y = -0.05\ m/s$. From thereon, the velocities of the particles in all three dimensions changed with time, due to their contact with each other and the screen surface. The numbers of particles created, their creation rate, their spatial position and their material properties were specified in the particle factory, positioned above the feeder. For even mixing

and avoidance of packing complications, the dynamic particle option was selected (in EDEM) as it is more efficient than the static method (Bbosa 2013).

Table 3.1: DEM modelling conditions

Material properties	**Poisson's ratio**	**Shear modulus**	**Density**
Particles	0.3	23 MPa	2678 kg/m^3
Screen	0.29	79.92 GPa	7861 kg/m^3
Collision properties	**Coefficient of restitution**	**Coefficient of static friction**	**Coefficient of rolling friction**
Particle-particle	0.1	0.545	0.01
Particle-screen	0.2	0.5	0.01
Particle diameter	3 mm and 5 mm	Particle generate rate	7000 particles/s
Variable	**Test Value**		
Screen aperture (mm)	3.5		
Angle of declination (deg)	25		
Vibration amplitude (mm)	1.0, 1.5, 2.0, 2.5		
Vibration frequency (Hz)	4, 6, 8, 10, 12		
Screen vibration	Sinusoidal translation		
Particle size (mm)	Binary size distribution (50% by volume of oversize and undersize) for each type of screen		

The Hertz-Mindlin (no slip) contact model (Mindlin and Deresiewica 1953) discussed in section 2.5.1 was employed to simulate particle-particle and particle-geometry interactions. This model is based on Hertz's theory and Mindlin's no-slip improved model in the normal and shear directions, respectively. The amount of time between successive iterations (time step) in the simulation was carefully chosen to avoid incorrect calculation of particle contact forces and interactions. To ensure stability in the system, the time step was set to at least half of the critical time step as suggested by DEM-Solutions (2006) and Bbosa (2013). According to DEM-Solutions (2006), the critical time step (also known as the Rayleigh time) is the time taken for a shear wave to propagate through a solid particle. The time step employed in this work was $1.83 \times 10^{-6}s$ (DEM-Solutions 2006). Analysis of the flow was done at an accumulated average time intervals of $0.5s$. The snapshots of the flow at this time interval are shown in Figure 3.2.

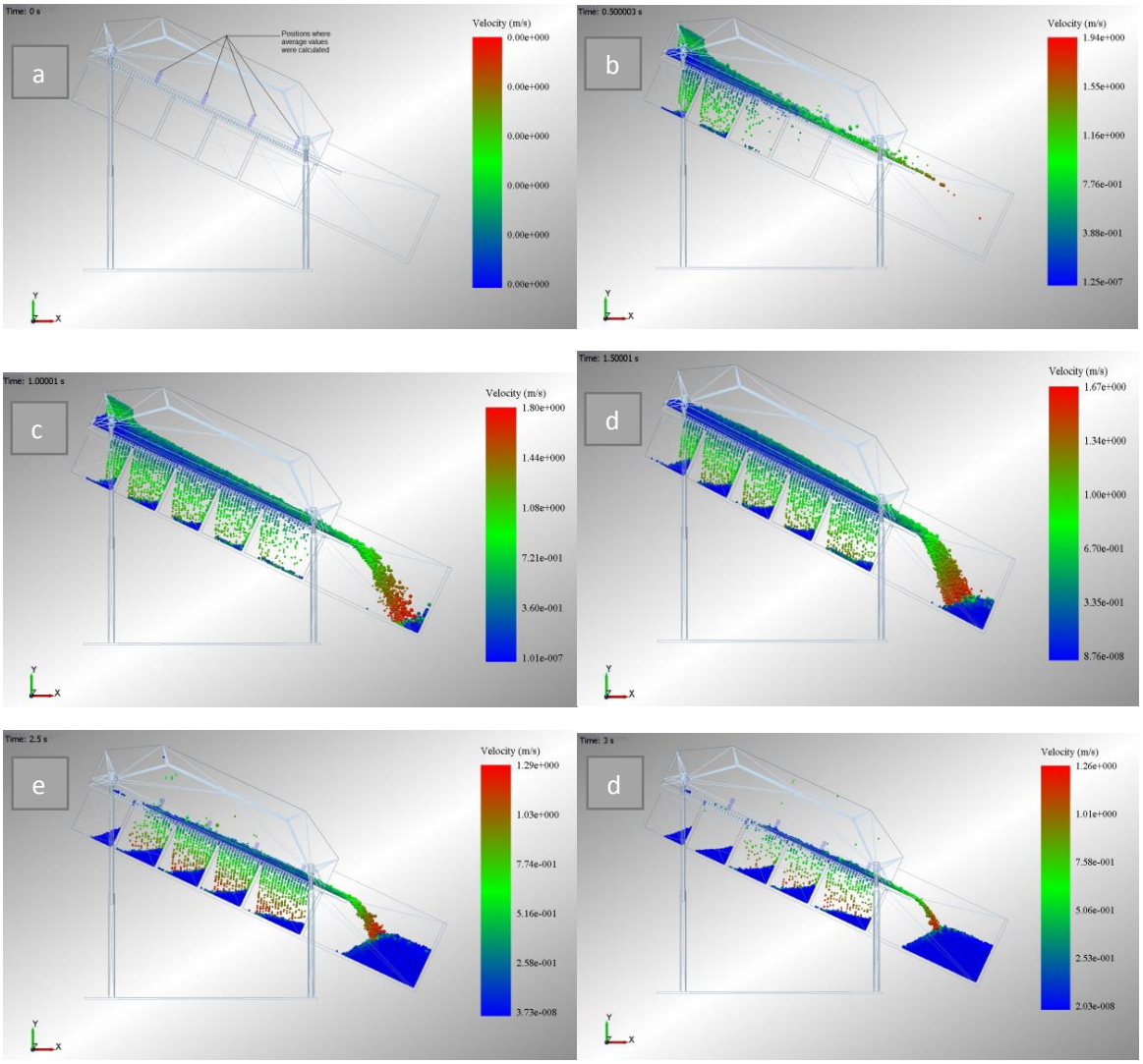

Figure 3.2: Particle motion on the screen at $0.5s$ intervals. a shows when $t = 0s$ and positions where average values of flow where calculated. $b - d$ show particle motion from $0.5s$ to $3s$ at $0.5s$ intervals

3.2 Data processing

3.2.1 Statistics: Coarse-graining

The use of a proper and accurate micro-macro transition method helps to transfer a discrete particle system to a corresponding continuum model (Zhu et al. 2007). To formulate an accurate continuum model, numerical or experimental data are required to calibrate and validate the model. In this work, discrete particle simulation data were extracted both to confirm the

assumptions of and provide the required closure rules for the rheological model to characterise the granular flow on a vibrating inclined screen. The averaging method employed in this study was the coarse-graining method. This method has been employed to study the constitutive behaviour of granular matter, and the micro-dynamical behaviour of granular flow (Zhu et al. 2007; Glasser and Goldhirsch 2001; Zhu and Yu 2002). The combined approach of discrete and averaging procedures gives a better understanding of the basic mechanisms of granular flows. Global assumptions are not required as the combined approach takes into account the discrete nature of the granular materials. This is a convenient way of analysing DEM simulation results to achieve continuum modelling suitable for engineering application.

In order to extract continuum fields from the discrete particle data, the coarse-graining approach described by Tunuguntla et al. (2015), Weinhart et al. (2012) and Glasser and Goldhirsch (2001) was employed. According to Weinhart et al. (2012), this approach is appropriate to analyse the continuum model in this work because the fields produced automatically satisfy the equations of continuum mechanics, even near the base of the flow. Compared to other methods described in the literature Luding and Alonso-Marroquín (2011), Weinhart et al. (2012), and the cited references therein, the coarse-graining method is most suitable because:

(i) the resulting macroscopic fields satisfy the continuum mechanics equation even close to the boundaries; and

(ii) no averaging over several time steps is required, i.e the resulting field is valid even for a single time step.

Furthermore, other methods apply essentially to a homogenous and steady situation, because an ensemble-averaging is required to obtain accurate results (Tunuguntla et al. 2015). The Coarse-graining method on the other hand, uses a smoothing kernel (coarse-graining function), which automatically generates fields satisfying the continuum equations. In this work, the coarse-graining approach of Tunuguntla et al. (2015) was applied to bi-disperse spherical glass beads on a vibrating screen system. From Figure 3.3, the two constituents are seen to appear simultaneously at every point on the screen. Hence, at each point in space and time,

the particle velocities associated with each constituent overlap.

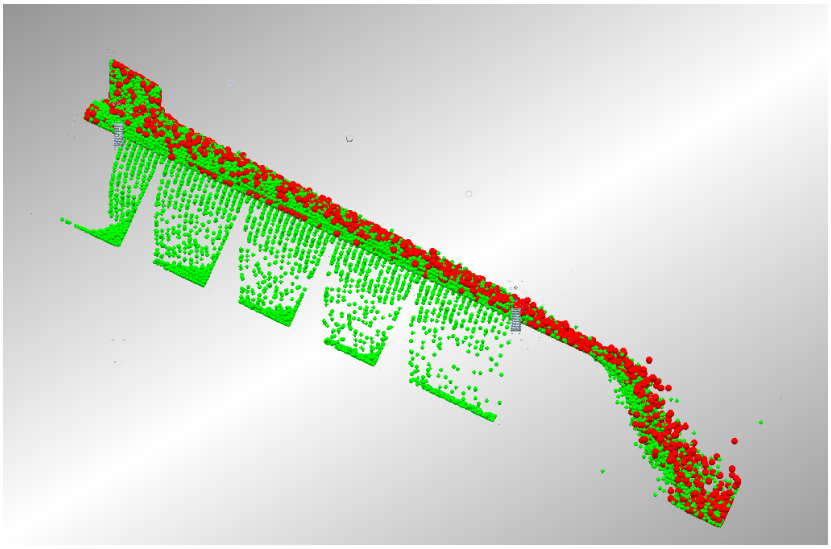

Figure 3.3: A snapshot of bi-disperse particle flow on an inclined vibrating screen from a simulation carried out in this work. The screen is inclined at 25° to the horizontal. The red and green particles are the two particle constituents i considered in this work. S is the bulk constituents of the flow, S^1 and S^2 are bulk constituents type 1 and 2 respectively, where $i \in S$ and $S = S^1 \cup S^2$

For spherical particles of radius a_i, the centre of mass is represented as $\vec{r}_i$, the mass as m_i and the velocity as $\vec{v}_i$. Figure 3.4 depicts two particle constituents i and j in contact with each other. For each constituent pair, the contact vector $\vec{r}_{ij} = \vec{r}_i - \vec{r}_j$, and the unit vector $\vec{n}_{ij} = \frac{\vec{r}_{ij}}{|\vec{r}_{ij}|}$ (pointing from j to i). Further to this, the overlap between the two particle constituents is expressed as $\delta_{ij} = max(a_i + a_j - \vec{r}_{ij}.\vec{n}_{ij}, 0)$, and the contact point and branch vector as $\vec{c}_{ij} = \vec{r}_i + (a_i - \delta_{ij}/2)/\vec{r}_{ij}$ and $\vec{b}_{ij} = \vec{r}_i - \vec{c}_{ij}$ respectively.

For a set of centre-of-mass coordinates $\vec{r}_i(t); \vec{v}_i(t); m_i$, the statistical mechanical definitions for microscopic mass density and momentum are expressed as:

$$\rho^{mic}(\vec{r}, t) \equiv \sum_i m_i \delta[\vec{r} - \vec{r}_i(t)] \tag{3.1}$$

and

$$\vartheta^{mic}(\vec{r}, t) \equiv \sum_i m_i \vec{v}_i(\vec{r}, t) \delta[\vec{r} - \vec{r}_i(t)] \tag{3.2}$$

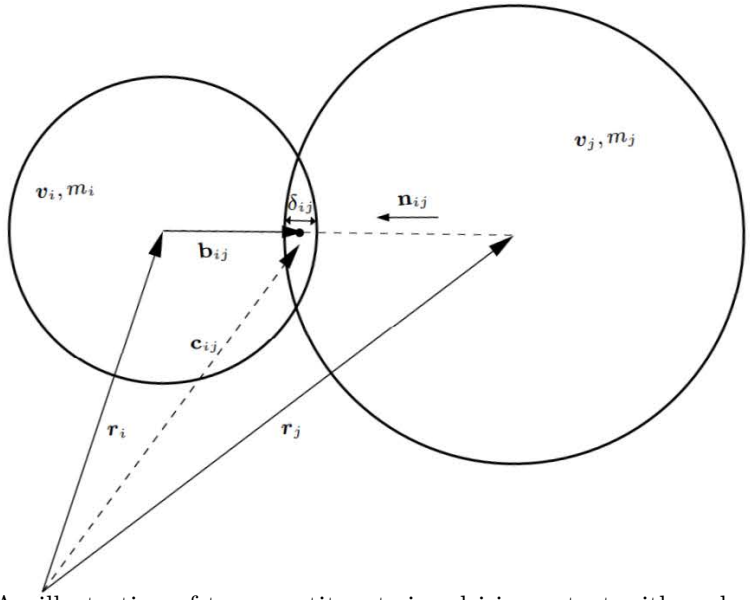

Figure 3.4: An illustration of two constituents i and j in contact with each other. Reproduced from Tunuguntla et al. (2015)

where m_i denotes the mass of particle i, and the corresponding position of the centre of mass of the particle at time t is denoted by $\vec{r}_i(t)$. The corresponding centre-of-mass velocity is $\vec{v}_i(t) \equiv \vec{r}_i(t)$. The relative positions of the centres of mass of two particles is $\vec{r}_{ij} \equiv \vec{r}_i(t) - \vec{r}_j(t)$ and the corresponding relative centre-of-mass velocities is $\vec{v}_{ij}$. For a bi-disperse system of type 1 and 2, and bulk constituents set $S^1 \cup S^2$, equation 3.1 is expressed as:

$$\rho^{mic,\beta}(\vec{r},t) \equiv \sum_{i \in S^\beta} m_i \delta[\vec{r} - \vec{r}_i(t)] \tag{3.3}$$

where β is type 1 and 2. According to Glasser and Goldhirsch (2001), the delta-function is a Dirac function defined in 3-dimensional Euclidean space R^3. Since the summation of the mass density of a volume in space equals the mass of all the particles in the volume, equation 3.3 can be convoluted with a spatial grain function $\psi(r)$ also known as a smoothing function. Hence,

$$\rho^{\beta}(\vec{r},t) = \sum_{i \in S^\beta} \int_{R^3} \rho^{\beta,mic} \psi(\vec{r} - \vec{r}\prime) d\vec{r}\prime = \sum_{i \in S^\beta} m_i \psi[\vec{r} - \vec{r}_i(t)]. \tag{3.4}$$

The smoothing function $\psi(r)$ possesses the following properties:

(i) It is non-negative semi-definite, i.e $\psi(\vec{r}) \geq 0$ (as such, the density field is positive).

(ii) The integral over space is normalized, i.e $\int_{R^3} \psi(\vec{r}) d\vec{r} = 1$, guaranteeing the conservation of mass and momentum.

The smoothing function $\psi(r)$ possesses a predetermined width w which is the coarse-graining scale. The value chosen for w in this work was 0.005 m which was the diameter of the bigger particle. The goal was to obtain a kernel density estimation of a finite data sample within the probe region, including where no data are observed. The contribution of each data point was smoothed out and the aggregate of the individual smoothed contributions gives an overall picture of the structure of the data. In this work, ψ was taken as a Gaussian of width w. The choice of a Gaussian allows for a smoother resulting field, similar to the observation of Goldhirsch (2010).

In Figure 3.5, the probe point r is highlighted in red. The probe point is tilted such that it is perpendicular to the flow and cuts across the width of the screen. The position of particles is not stationary, but changes with time t as particles move along the screen. The movements of particles are tracked in 3D as vector r_i where i is in $[x, y, z]$. A single probe position is enough (MiDi 2004; Tunuguntla et al. 2015) as all particles pass through this point provided readings are taken from time $t = 0s$. Data exported from the simulation results to models in equations 3.4 and 3.9 include the positions $\vec{r_i}$ and velocities $\vec{v_i}$ of individual particle constituents at different time steps (Figure 3.2). Other parameters are mass m_i, and average particle diameter d. From these primary data, analyses are carried out in MATLAB for the derivation of the partial density and the partial momentum density.

An essential parameter to quantifying the rheology in this work is the volume fraction ϕ, which was calculated for the two constituents separately and jointly. Measurements were taken at steady flow, in line with MiDi (2004) and Tunuguntla et al. (2015). The total volume fraction is represented by ϕ^β where β represents large and small particles and the interstitial fluid (air). These particle types can be expressed as a bulk constituent of set $S^1 \cup S^2$ where each

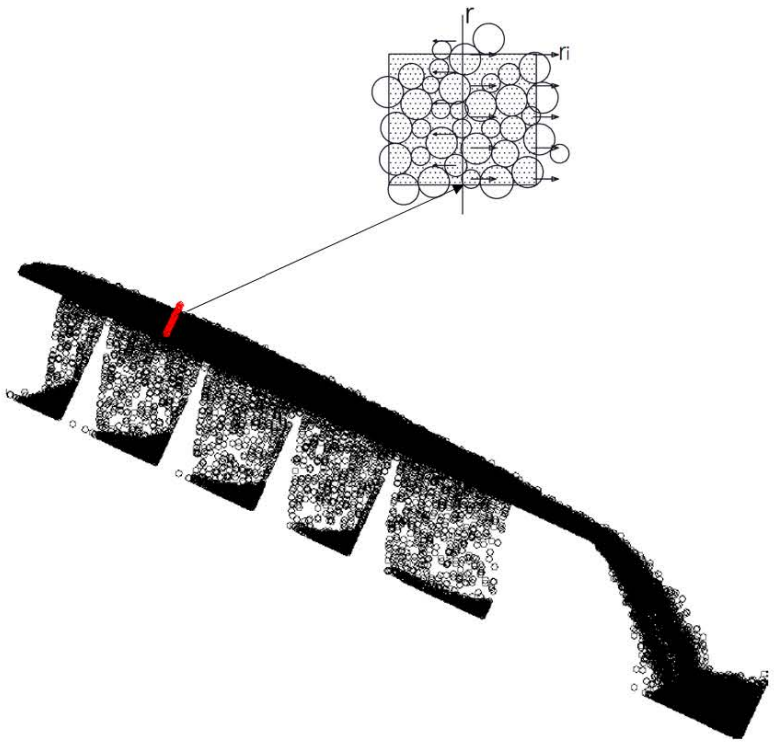

Figure 3.5: Kernel density estimate. The red line is the depth at which readings were taken at different time steps in this work. The inset shows particles movements from the reference point r and the flow of particles in 3- dimension r_i where $i = x, y, z$

constituent $i \in S$. The smoothing kernel function is applied to calculate the volume fraction, the depth of flow at point x, and time t. The granular flow in a vibrating screen is divided into a mixture of large and small particles, whose interstitial fluid is air in the case of dry screening. At the initial stage when particles are fed to the screen, every point is simultaneously occupied by the three phases, i.e. small and large particles and the passive fluid (air). As screening begins, segregation and percolation of the small particles occurs along the screen, leaving a higher concentration of the large particles.

Given each constituents β, we define the overlapping partial density, partial velocity and partial pressure as ρ^β, $\vec{u}^\beta$, and P^β respectively. Constituent $\beta = l + s + \mathbf{a}$, where l represents large particles, s represents small particles, and $\mathbf{a}$ is the passive fluid (air). Each constituent

occupies a volume fraction ϕ^{β} per unit volume and

$$\phi^{l} + \phi^{s} + \phi^{\mathbf{a}} = 1 \tag{3.5}$$

Ignoring the passive fluid, the volume fraction of grains per unit mixture is

$$\phi^{\mathbf{g}} = \phi^{l} + \phi^{s} \tag{3.6}$$

The volume concentration of large and small particles per unit volume are

$$\phi^{\Upsilon} = \phi^{\Upsilon}/\phi^{\mathbf{g}}, \tag{3.7}$$

where $\Upsilon = l$, s which also sum up to unity. i.e $\phi^{l} + \phi^{s} = 1$

The corresponding volume fractions are calculated as follows:

$$\phi^{\beta} = \frac{\rho^{\beta}}{\rho_{p}^{\beta}} \tag{3.8}$$

where ρ_{p}^{β} is the material density of constituent type β and ϕ^{β} is the bulk volume fraction.

The methodology described above was applied to analyse the results from the simulations of the flow of binary mixtures of two particle sizes 3 mm and 5 mm, on a vibrating screen with square apertures.The near-size problem was factored in (i.e. when the particle size is close to that of the screen aperture) to see how this affects the particle flow on the screen and the percolation of undersize particles. This started with the flow on the screen and the resulting Eulerian fields that form the basis for developing continuum-type modelling.

Further to obtaining the volume concentrations as discussed above, the velocity fields which are arguably the most important quantities for continuum modelling were obtained from the ratios of the partial momentum and mass density fields (equations 3.11-3.12), as explained below.

For constituents type β The coarse-grained partial momentum density is given by,:

$$\vec{\vartheta}^{\beta}(r,t) = \Sigma_{i \in S^{\beta}} m_i \vec{v}_i \psi_i \tag{3.9}$$

$$\vec{u}^{\beta} = \frac{\vec{\vartheta}^{\beta}(\vec{r},t)}{\rho^{\beta}(\vec{r},t)} \tag{3.10}$$

where u^{β} is the average velocity.

3.2.2 Scaling relations

Well formulated scaling laws will help to unravel the governing mechanisms of multi-directional flows on and through a vibrating screen. In an attempt to describe experimental results quantitatively, Jop et al. (2006) showed that the depth-averaged velocity varies as the thickness of the granular layer to the power of 3/2. This scaling, otherwise known as Bagnold's scaling, comes naturally from dimensional analysis in the absence of basic time scales. One might expect that most studies would observe this kind of rheology; however, results strongly depend on the experimental procedure (Silbert et al. 2003).

In the case of a vibrating screen, the boundary conditions, which involve the vibrational intensity of the geometry, complicate a direct quantitative comparison with the experiments. For instance, the average velocity along the screen, the depth of granular flow, and the solids concentration behave differently along a vibrating inclined plane.

In fluid dynamics, the Froude number, F_r, is the ratio of two dominant forces, the inertial force and the weight force, i.e. $F_r = \frac{\upsilon}{\sqrt{gL}}$, where L and υ are the characteristic length dimension and characteristic velocity of the system, respectively (Hilden 2007). In granular flow, an analogous expression can be used to describe the bed velocity in dimensionless terms (MiDi

2004):

$$F_r(velocity) = \frac{\text{average velocity of the particle bed}}{\sqrt{g.(\text{amplitude of vibration})}} = \frac{\langle v \rangle}{\sqrt{g.R}} \tag{3.11}$$

For a vibrating screen surface,

$$F_r(vibration) = \frac{(\text{peak velocity of vibrating surface})^2}{g.(\text{amplitude of vibration})} = \frac{(R\omega)^2}{g.R} = \frac{R\omega^2}{g} = \frac{R.(2\pi f)^2}{g} = \Gamma \tag{3.12}$$

where R and ω are the vibration amplitude and angular frequency, respectively. R can be replaced by the depth of flow of particles on the screen, h, or particle diameter, d (Meinel 1998). The measure of the vibratory motion characteristics is the throw value (intensity of vibration, jump index, or g - force), Γ, which is the peak acceleration of the screen.

Γ is a dimensionless number combining the acceleration due to gravity, g, the vibration frequency, f, and the amplitude of vibration, R. Other dimensionless parameters include the scaled average depth, $\frac{h}{d}$, defined above, and the scaled flow rate, Q, of the particles on the screen, given as :

$$Q = \int \langle v \rangle \delta \langle h \rangle. \tag{3.13}$$

For an inclined plane geometry, the parameter I is constant everywhere across the system; likewise, the shear rate $\dot{\gamma}$ is uniform and the predicted velocity profile is linear (MiDi 2004). At the wall, the effective friction coefficient obeys the rheological law, i.e $\frac{\tau_w}{p_w} = \mu(I)$ (see details in Chapter 2). While this law applies favourably to a dense flow, it tends to change when the flow becomes collisional. (In Chapter 4, a stress model is formulated that classifies the flow in an inclined vibrating screen geometry into three regimes, each dominated by a corresponding stress (contact, collisional, and turbulence stress). The transition between the regimes is investigated through the dimensionless parameter I.)

The flow layer is essential to developing a scaling relation between the flow rate and the flow

depth in a free surface flow system. The velocity as a function of position in an inclined plane geometry is :

$$V(y) = \int_0^h \dot{\gamma}(y)dy \tag{3.14}$$

and the stress distribution is:

$$P = \rho g(h-y)cos(\theta), \tag{3.15}$$

with

$$\frac{\tau}{P} = tan(\theta) \tag{3.16}$$

,

where θ is the angle of inclination of the screen (see Figure 2.5).

The shear rate $\dot{\gamma}$ is defined by the relationship;

$$\dot{\gamma}(y) = \frac{1}{d}\sqrt{\frac{P(y)}{\rho}}\mu^{-1}(tan(\theta)) = \frac{1}{d}\sqrt{g(h-y)cos(\theta)}\mu^{-1}(tan(\theta)). \tag{3.17}$$

Integrating equation 3.14 over the depth of flow, and scaling with the factor $\sqrt{gd}$, gives a velocity profile in the form:

$$\frac{V(y)}{\sqrt{gd}} = A(\theta)\frac{3}{2}\frac{[h^{3/2} - (h-y)^{3/2}]}{d^{3/2}} \tag{3.18}$$

where

$$A(\theta) = \frac{2}{3}I(\theta)\sqrt{cos(\theta)} = \frac{2}{3}\mu^{-1}(tan(\theta))\sqrt{cos(\theta)} \tag{3.19}$$

The average velocity $\langle V \rangle$ can be analysed as:

$$\frac{\langle V \rangle}{\sqrt{gd}} = \frac{1}{h}\int_0^h \frac{V(y)}{\sqrt{gd}}dy = \frac{9}{10}A(\theta)\left(\frac{h}{d}\right)^{3/2} \tag{3.20}$$

The velocity in this case scales with the depth of flow to the power 3/2, and is otherwise called the Bagnold profile. It is important to note that the Bagnold profile relies on dimensional reasoning and not on collisional arguments.

Much empirical work has been done to investigate the scaling relation between the velocity of flow and the depth of flow in an inclined plane configuration. These experiments essentially focus on how changing flow parameters can affect the scaling ($\langle V \rangle$ versus h) in the system. These parameters range from changing the bed conditions to the influence of material types on the flow. However, no unified scaling description emerges from the different experiments (Pouliquen 1999b; Pathmathas 2015).

Silbert et al. (2001) observed that the velocity in the direction of flow (V_x) scales with the depth of flow according to $V_x(y) \propto h^n$ where $n = 1.52 \pm 0.05$. The shear rate $\dot{\gamma}$ in these cases depends on the flow rate Q. In this work, the flow rate was re-scaled as:

$$Q^* = \sqrt{\frac{\langle V \rangle}{d\sqrt{gd}}} \tag{3.21}$$

3.2.3 Scaling relations obtained in this work

Figures 3.6 and 3.7 reveal a different scaling relation for this work, which is not surprising as the configuration of an inclined vibrating screen is different from that of an inclined plane. The granular flow in this system is influenced by both the angle of inclination (θ) and the vibration intensity (Γ). Due to the vibrating surface, the particles do not flow steadily down the screen hence the scaling relation will be different from the Bagnold's profile in other free surface flow (such as inclined planes, heap flow, and rotating drums). Further, the screening effect (i.e. percolation of undersize particles through the aperture of the screen) and the binary flow of particles are additional factors that determine the depth and the average velocity of the flow.

In Figures 3.6 and 3.7, the re-scaled flow rate and the scaled average velocity are plotted against the scaled depth (h/d) for different intensities of vibration of the screen. The best fitting power law for the re-scaled flow rate $\left[\sqrt{Q^*} = a(h/d)^n\right]$ yields $n = 0.239 \pm 0.03$, while for the scaled average velocity $\left[\frac{\langle V \rangle}{d\sqrt{gd}} = a(h/d)^n\right]$, $n = 0.4017 \pm 0.03$. The scaling allows for the testing of the underlying scaling relation. While these results are different from those

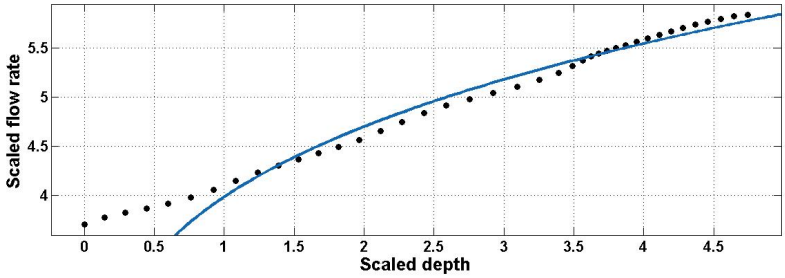

Figure 3.6: Variation of the re-scaled flow rate $\left(\sqrt{Q^*}\right)$ with scaled depth (h/d)

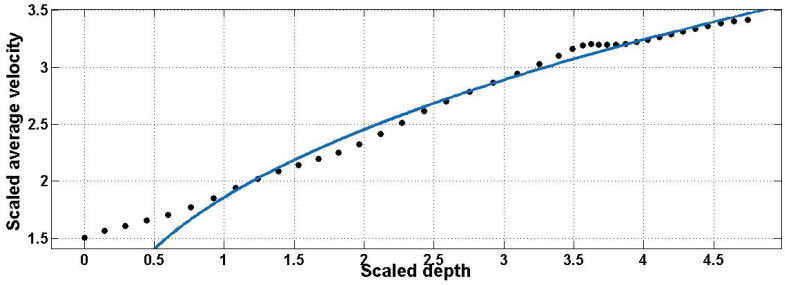

Figure 3.7: Variation of the scaled average velocity $\left(\sqrt{\frac{\langle V \rangle}{\sqrt{gd}}}\right)$ with scaled depth (h/d)

of inclined plane free surface flow, they are similar to those of rotating drums. Table 3.2 summarises different scaling relations obtained for different geometries of flow. A comparison with flow in a rotating drum is probably more appropriate for a vibrating inclined screen since they are both free surface flow and are both affected by the motion of the geometry (MiDi 2004).

Table 3.2: Scaling laws for the variation of scaled flow rate with scaled flowing layer depth for open surface flow geometry

Author	**Scaling:$\langle V\rangle$ versus h**	**Estimated $\lvert\dot{\gamma}\rvert$**	**Comments/Definitions**
Parker et al. (1997)	$\langle V\rangle \propto h^0$	≈ 0	excessive wall slip
Orpe and Khakhar (2001)	$\langle V\rangle \propto h^3$	$\sqrt{\frac{g\omega}{Md\cos(\theta)}}$	M $\equiv$ fit parameter; $\theta \equiv$ repose
MiDi (2004)	$\langle V\rangle \propto h$	$\dot{\gamma} \approx 0.5\sqrt{\frac{g}{d}}$	wide range of data
Jop et al. (2006)	$\langle V\rangle \propto h^{3/2}$	depends on Q^*	based on heap flows
Felix et al. (2007)	$\langle V\rangle \propto h^n$	variable	$n = 5.5 \pm 0.5$ for $\frac{D}{d} = 100$
Pignatel et al. (2012)	$\left[\frac{h}{d} = 2.86\left(\frac{\langle V\rangle h}{d\sqrt{dg}}\right)^{0.44}\right]$	variable	best fitted power law (all data)
Pathmathas (2015)	$\langle V\rangle \propto h^{0.86}$	$\dot{\gamma} \approx 0.25\sqrt{\frac{g}{\langle d\rangle}}$	$n = 0.86 \pm 0.04$; $\langle d\rangle = 6.5$ mm
In this work	$\langle V\rangle \propto h^{0.40}$	variable $\dot{\gamma}$ at constant fit of $\approx 1.7\sqrt{\frac{g}{\langle d\rangle}}$	$n = 0.40 \pm 0.03$ for $\langle d\rangle =$ 4 mm

3.3 Summary

This chapter reported the conditions for simulations using DEM and the micro-macro transition method employed in this work. This method is otherwise called coarse-graining. Granular mixtures of two particle constituents were simulated on an inclined vibrating screen using the commercial DEM package EDEM, developed by DEM solutions.

The modelling conditions and geometry parameters have been discussed in this work. The information extracted from the discrete particle simulation was used both to confirm the assumptions of and provide the required closure rules for a rheological model to characterise the granular flow on an inclined vibrating screen. While microscopic properties were employed for the simulation, the properties extracted from the simulation are macroscopic fields which are consistent with the continuum equations of mass, momentum, and energy balance.

From the continuum equations, the volume fraction and the tangential velocity as a function of the depth of flow along the inclined surface were derived. Data were extracted when the system attained a steady flow. The velocity and volume fraction distribution delineate different flow

regimes in the flow. These flow regimes make it difficult to obtain a clear constitutive choice for the shear stress. By fitting the average scaled flow rate and the tangential velocity data to the normalised depth, scaling relations of the form $[\sqrt{Q^*} \propto (h/d)^n]$, where $n = 0.239 \pm 0.03$, and $[\langle V \rangle \propto (h/d)^n]$, where $n = 0.4017 \pm 0.03$, were obtained for the flow rate and velocity respectively. These values were the closest when compared to similar results in the literature (Table 3.2) for free surface flow. Although, these values are not exactly the same as the Bagnold's profile, a similar relationship occurs between the average flow velocity and the depth of flow. The Bagnold's profile value of 3/2 is for an ideal case of a steady flow down and inclined plane without vibration. In this geometry (vibrating screen), granular flow is influenced by both vibration and the inclination of the screen hence, the difference in the scaling relations from the Bagnol's profile.

Chapter 4

Vibrating Screen Rheology

4.1 Introduction and motivation

The need to identify the dominant stresses in a vibrating screen has informed the decision to characterise the granular flow during screening in this work. This chapter presents the development of an effective frictional coefficient model that is based on frictional, collisional-kinetic, and turbulent stresses. The quasi-static regime is dominated by frictional stress, and corresponds to low inertial number, (I) (Jop et al. 2005; Taberlet et al. 2003). In this work, the frictional stress is divided into internal and wall shear stress. Beyond the quasi-static regime, the frictional stress chains break and the collisional-kinetic and the turbulent stresses begin to dominate.

In section 2.6 above, it was shown how the combination of the kinetic and static stresses yields an effective friction coefficient $\mu(I)$ that captures the hysteresis from the start of flow down an inclined plane to the end of the steady state, and the transition that must occur from the dense (liquid-like) regime to a gaseous-like regime. Lee and Huang (2012) observed a kinetic stress in the flow as a result of the transition from liquid-like flow to gas-like flow. Their model successfully captures the hysteresis at the flow initiation and the transition from liquid-like to gas-like flow (Figure 2.9). However, a sharp discontinuity in the model suggests

a deficiency which the authors suggested should be investigated. Intuitively, the transition from the liquid-like to the gas-like regime should correspond to a net decrease in the effective friction coefficient because of the dilute nature of the flow. Lun et al. (1984) and Jop et al. (2006), using kinetic theory and visco-plastic rheology, agree that the effective friction coefficient decreases or should break down for high values of the inertial number, I.

While the model of Lee and Huang (2012) is able to capture the crucial transitions in the system, the hypothesis in this work will test if the inclusion of a turbulent regime in the flow, and an appropriate solids concentration (ϕ) that varies with inertial number (I), can correct the deficiency in the system. Further, a model of the effective friction coefficient should capture the transition between three phases, namely: solid-like, the liquid-like, and the gas-like regimes which are described in this work as the quasi-static, kinetic, and turbulent regimes. To characterise the flow, this work notes that each regime of flow is dominated by a corresponding stress. Further to this, different regimes of flow are identified by their solids concentration.

4.2 Model formulation

As discussed in Chapter 3, the flow behaviour of granular materials can be predicted by solving the average balance equations obtained from the continuum mechanics approach. Due to their discrete nature, the microscopic interactions of individual particles are used to describe the bulk flow in DEM. As shown in Figure 4.1, for a fully developed granular flow down an inclined plane, u_1 denotes the velocity in the direction of flow, and u_2 is the velocity perpendicular to the direction of flow, where x_1 and x_2 are the parallel and the perpendicular axes to the plane, respectively, and θ is the angle of inclination of the bed. The dotted line represents the maximum depth of flow across the screen. P and τ are the normal stress (pressure) and the shear stress, respectively.

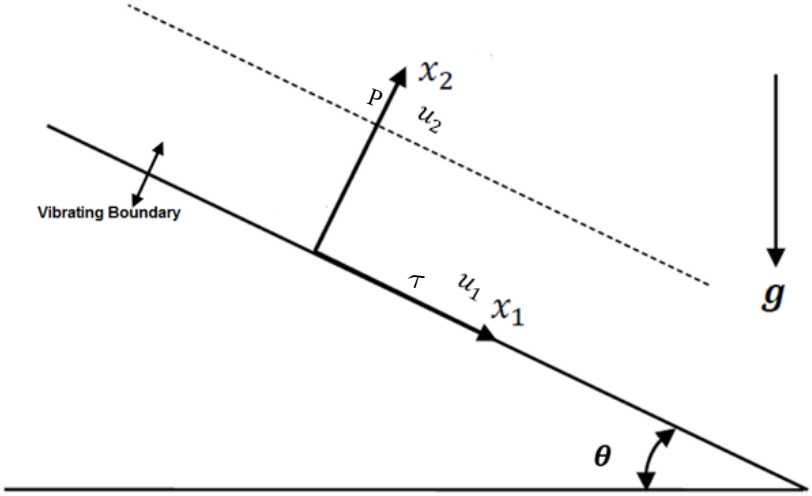

Figure 4.1: Coordinate system for the flow down an inclined screen

The conservation of mass for the flow is given by:

$$\frac{D(\rho_p \phi^\beta)}{Dt} + \rho_p \phi^\beta \frac{Du_i}{Dx_i} = 0 \tag{4.1}$$

where i is the direction of velocity. The momentum equations are given by:

$$\frac{D(\rho_p \phi^\beta \vec{u}_1)}{Dt} = \frac{-D(\rho_p \phi^\beta \vec{u}_1 \vec{u}_2)}{Dx_2} + \frac{D\tau_{1,2}}{Dx_2} + \rho_p \phi g \sin\theta \tag{4.2}$$

and

$$\frac{D(\rho_p \phi^\beta \vec{u}_2)}{Dt} = \frac{-D(\rho_p \phi^\beta \vec{u}_2 \vec{u}_2)}{Dx_2} - \frac{DP}{Dx_2} - \rho_p \phi^\beta g \cos\theta \tag{4.3}$$

The flow regimes observed in this system are characterised by the volume fraction and velocity. At low velocity and high solids concentration, when the particles deform slowly, the flow is dominated by frictional force and contact stress (static stress). As particles gain momentum, they move faster, and collide randomly with each other and with the wall. This motion causes dilation in the flow such that the particles begin to behave like a molecular gas. At this point, the kinetic stress is dominant. As in kinetic theory, the particle velocity

can be decomposed into time-averaged and fluctuating velocity components (Clement and Rajchenbach 1991). Analogous to the thermodynamic temperature is the granular temperature T which represents the energy associated with the random motion in the kinetic regime. In addition to the volume fraction ϕ^β and the velocity $\vec{u}^\beta$, in the momentum equations 3.2 and 3.3, the granular temperature, given as $T = \frac{1}{3}(\langle \grave{u}_1^2 \rangle + \langle \grave{u}_2^2 \rangle + \langle \grave{u}_3^2 \rangle)$, can also characterize the local state of the granular material, where $\grave{u}_i$ is the fluctuating velocity with a zero time average and $\langle\rangle$ represents an ensemble average.

As previously discussed in sections 2.6 and 4.1, the order of the inertial number I from small to large values corresponds to the change in flow behaviour from the quasi-static regime to the kinetic-collisional regime, and the turbulent regime. To capture the effects of the quasi-static (τ_s), the kinetic-collision (τ_c) and the turbulent (τ_t) shear stresses, this work assumes that the shear stresses obey the additive rule (Lee and Huang 2012; Shuyan et al. 2009) such that the total stress can be expressed as:

$$\tau = \tau_s + \tau_c + \tau_t. \tag{4.4}$$

τ_s can be substituted with the sum of the internal shear stress τ_i and the side wall frictional shear stress τ_w, so

$$\tau = \tau_i + \tau_w + \tau_c + \tau_t. \tag{4.5}$$

Similarly, the pressure is made up of the quasi-static, kinetic-collision, and the turbulent pressure, i.e.

$$P = p_s + p_c + p_t, \tag{4.6}$$

where p_s, p_c and p_t are the quasi-static, the collisional-kinetic, and the turbulent normal stress (pressure) respectively. Corresponding to the quasi-static shear stress, the quasi-static normal stress can be expressed as the sum of p_i and p_w. τ and P are thus derived to capture the essential flow regimes observed in the system. The frictional stress essentially relies on

the internal shear stress between particles and the side wall frictional stress. All possible contact frictions in relation to the flow are considered in order to derive a total effective friction between the flowing layer and the geometry.

MiDi (2004) and Jop et al. (2006) observed that the flow of granular materials on an inclined plane depends on the angle of inclination. In their systems, the inclination angle determines the effective frictional coefficient between the flowing layer and the rough bottom. In an inclined vibrating screen geometry, other factors such as vibration intensity, size of particles, and aperture size contribute to granular flow. Although the model developed in this work does not factor in all screening parameters, the effect of each parameter on the volume concentration and the shear rate determines the flow regime. The influence of each parameter will affect the effective frictional coefficient as I changes.

4.2.1 Pressure, volume fraction and bulk density

The inertial number I is defined as $I = d\dot{\gamma}/\sqrt{P/\rho_p}$, where d is the average particle diameter, $\dot{\gamma}$ is the shear rate, and ρ_p is the particle density. From the inertial number I, the confining pressure P can be expressed as:

$$P = \rho_p \left(\frac{d\dot{\gamma}}{I}\right)^2. \tag{4.7}$$

I is an essential dimensionless parameter that controls the transition from one regime of flow to another. In fact, I controls the flow (see section 2.6). As I increases, the flow evolves from a quasi-static regime to a dilute regime and then to a collisional regime. Equation 4.8 expresses the total pressure P as inversely proportional to I which implies that high values of I correspond to low P and vice versa. As discussed in section 4.1, low values of I correspond to the quasi-static regime. If $p_s \to 0$ as I increases, it implies that $p_c + p_t$ should increase.

In a vibrating screen geometry, the granular flow exhibits an intermittent behaviour as transitions in the flow depend on the effect of the screening variables. While a quasi-static regime is

possible on a vibrating screen (as depicted in Figure 3.4), transition to collisional and possibly turbulent flow is inevitable. To achieve a total pressure P on a vibrating screen, I should be expressed in a way that spells out the effect of the transition on P. This pressure, which is pertinent only to moving media, also depends on the solids fraction of the media. During screening, periodic tapping and percolation of undersize particles vary the solids concentration and the bulk density along the screen. As discussed in section 3.2.1, and expressed by equation 3.8, the relationship between the bulk density ρ_β, the material density ρ_p^β, and the volume concentration ϕ^β is given by:

$$\rho_\beta = \phi^\beta \rho_p^\beta \tag{4.8}$$

Lee and Huang (2012) propose that p_s (the normal stress in the static regime) depends on the volume fraction ϕ and obeys the scaling law $p_s \sim p_o(\phi - \phi_{min})^\alpha$ at high loading [1] on an inclined plane without vibration. p_o and ϕ_{min} depend on the properties of the material while the value of α varies depending on the contact forces. Josserand et al. (2006) proposed $\alpha = 3/2$ for the Hertzian contact force employed in this work. This expression applies to a fully loaded (high and constant depth) granular flow on an inclined plane; the chances of achieving a fully loaded flow on an inclined vibrating screen are limited. Thus, in this work, another means of investigating the static normal stress for an inclined vibrating screen is derived. From equation 4.7,

$$p_s = P - p_c - p_t \tag{4.9}$$

From equation 4.9, it is important to first calculate P and subsequently p_c and p_t because at high values of p_c and p_t, p_s will vanish and negative values of p_s are not relevant (Lee and Huang 2012). In equation 4.7, the total pressure is expressed as a function of the shear rate and the inertial number, which implies that when $I \to 0$, the pressure will increase infinitely, which is not supported in literature. To overcome this dilemma, a more convenient approach adopted in this work is the dilatancy law[2] where the inertial number I is a function of the

[1] when particles are closely packed

[2] the variation of the mean volume fraction ϕ as a function of the inertial number I

volume fraction ϕ.

Different relationships apply to relating the volume fraction to the inertial number depending on the geometry and the conditions of flow. Hatano (2007) suggests a power law for the dilatancy such that $\phi(I) = \phi_{max} - aI^{\delta}$ for closely packed granular materials. The discrete element simulation was performed on granular layers subjected to isobaric plane shear. Jop et al. (2005) expressed dilatancy as a linear relationship where $\phi(I) = \phi_{max} + (\phi_{min} - \phi_{max})I$ for steady uniform granular flow on a static pile in a channel. Other forms of the relationships are the linear model of Da Cruz et al. (2005): $\phi(I) = \phi_{max} - aI$ for steady plane shear flow and the exponential decay function of Pathmathas (2015): $\phi(I) = \phi_{max} \exp(-bI^{c})$ for rotating drum. In the present study, an exponential decay function was employed because it captures the flow from the surface to the base. As explained by MiDi (2004), the rheological properties of free surface flow which include inclined plane shear flow, heap flow and rotating drum flow are similar. This study classifies vibrating screen flow as a free surface inclined flow. Further, granular flow down the screen decreases down the depth of flow despite the influence of vibration on the flow (see Figure 3.2).

To determine the maximum and minimum volume fractions, Figure 4.2 depicts the solids concentration profile across the granular bed of flow. Figure 4.3 delineates the various flow regimes observed in the flow and the volume concentration as a function of normalised depth at steady flow. The simulation results resented in Figures 4.2 to 4.5 are from the base case values where the frequency and the amplitude of vibration were constant (4 Hz and 1 mm respectively). The effects of the vibration intensity on the solids concentration and the effective friction are explained later in this chapter.

Points A, B, C, D, and E in Figure 4.2 are different transitions observed in the flow. Below point A is a region directly affected by the amplitude and the intensity of vibration of the screen. This region is highly fluidized, hence the reason for the low solids concentration. The

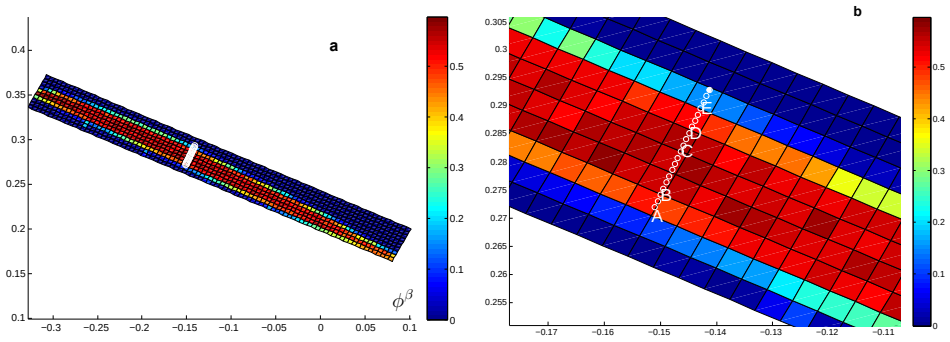

Figure 4.2: Variation of solids concentration ϕ across the bed of flow on a vibrating inclined screen. Below point A is a fluidized region directly affected by the vibration of the screen. Figure 4.2b shows zoomed-in image of Figure 4.a

volume fraction increases slightly from the screening surface to point A. The region between points A and B describes a static or plug-flow regime where the material velocity and the screen surface velocity are the same (Figure 4.3). In the quasi-static region, the solids concentration appears to increase slightly and then decreases when transforming from points C to D. Within the quasi-static region is the maximum solids concentration($\phi = \phi_{max}$). This corresponds to Jop et al. (2005)'s observations for inclined plane geometry.

Intuitively, one would expect point A to be fluidized as well, but the concentration of particles in this region is due to the segregation of the smaller particles finding their way to the screening apertures. Between points C and D, the particles are free to move around a little and hence behave like a liquid. Within this region, segregation occurs, but because of the screening process, the concentration decreases along the direction of flow. Between points D and E is the inertial regime[3] where the flow is dominated by both the inertial and collision forces. Above point E, some particles bounce off the screen at high vibration intensity which is an indication that there is turbulent stress in the inertial regime.

The quasi-static regime is dominated by frictional interaction. In this system, this regime is characterised by $\phi = \phi_{max}$ and is transient compared to the kinetic and the turbulent regimes. The value of $\phi_{max} = 0.58$ obtained in the base case (Figure 4.3) is very close to $\phi_{max} = 0.6$

[3]An instantaneous collisional regime observed in the flow in which collisions are binary and the flow is rapid. This regime is governed by both inertial and collisional effects and occurs close to the surface

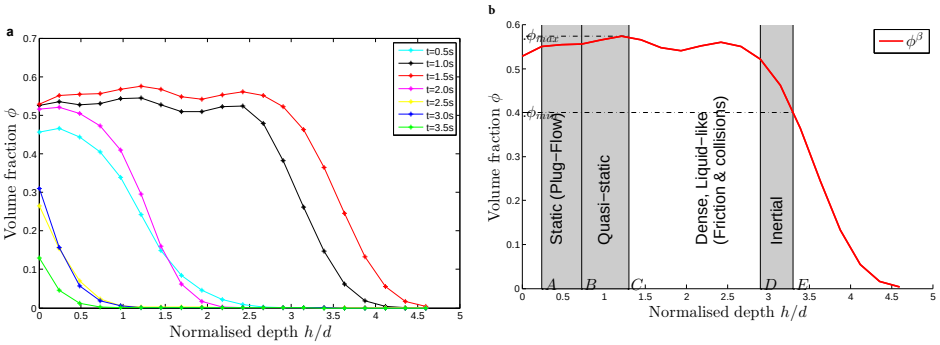

Figure 4.3: Solids concentration ϕ as a function of normalised depth (h/d). The profile is an expansion of points A - E in Figure 4.2. Figure 4.3a shows solids concentration at different time steps. The measurements employed in this work were taken at a steady flow when $t = 1.5s$. The various flow regimes are delineated in Figure 4.3b

observed by other workers in dense granular flow (Jop et al. 2006; Forterre and Pouliquen 2008). The choice of $\phi_{min} \approx 0.4$ is consistent with the original work of Bagnold (1954a). The region between $\phi_{max} < \phi < \phi_{min}$ is expected to be dominated by kinetic stress, as the stress chain of frictional interactions is expected to have broken within this region (Shuyan et al. 2009).

To estimate p_s in equation 4.9, the exponential decay function $\phi(I) = \phi_{max} \exp(-bI^c)$ is employed to determine the total pressure in the flow. This model is considered most appropriate because the bulk of the flow spans $0.2 < \phi \leq 0.58$ (Figure 4.4) for the inertial range of $10^{-3} \leq I \leq 1$. From the expression

$$\phi(I) = \phi_{max} \exp(-bI^c) \tag{4.10}$$

the total pressure P is derived as

$$P = \rho_p \left[\frac{d\dot{\gamma}}{(\frac{\ln \phi_{max} - \ln \phi}{b})^{1/c}} \right]^2 \tag{4.11}$$

The derivation of equation 4.11 satisfies I in equation 4.7 and, hence, the expression for the granular pressure P employed in this study. This work favours this pressure (equation 4.11)

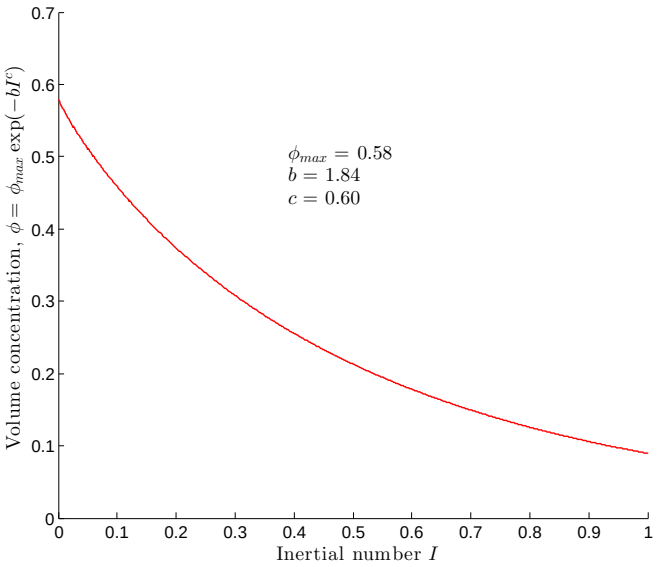

Figure 4.4: Variation of solids concentration with inertial number

over the hydrostatic pressure because the pressure beyond the quasi-static regime cannot be hydrostatic-like.

4.2.2 Stress components

After obtaining the expression for P, this section is concerned with developing an expression for the stress components. The stress components are essential for characterising the effective frictional flow. The rheological behaviour of the flow is characterised by the inertial number I and the effective friction $\mu(I)$. The effective friction is the ratio of the total shear stress τ to the total normal stress P (total pressure) i.e. $\frac{\tau}{P} = \mu(I)$. The total shear stress given by equations 4.4 and 4.5 is divided according to the flow regimes observed on the screen. The following expressions and analysis discuss the derivation of different stress components and the model for the rheological behaviour on the screen. As stated earlier in section 4.2, the quasi-static shear stress τ_s is composed of two contributions:

$$\tau_s = \tau_i + \tau_w \tag{4.12}$$

which are due to contact forces between particles and collisions with the wall. The first term τ_i is the internal frictional shear stress and the second term τ_w is the wall frictional shear stress (Jop et al. 2005; 2006; Taberlet et al. 2003). Jop et al. (2006), Orpe and Khakhar (2007), Lee and Huang (2012) and Pathmathas (2015) employed different rheological expressions for different geometries to argue that the internal frictional stress dominates the dense regime. In this work, the internal shear stress description of Jop et al. (2006):

$$\mu_i(I) = \mu_1 + \frac{\mu_2 - \mu_1}{I_0/I + 1} \tag{4.13}$$

was applied, where $I_0 = 0.279$, and μ_2 and μ_1 are constants that depend on the granular material. In the static region, $\tau_c + \tau_t = 0$, which implies that the only stress component evident in this regime is the static stress (τ_s). Likewise, the total pressure $P = p_s$ for the static regime. Since $\mu_i(I) = \frac{\tau_i}{P}$,

$$\tau_i = \left[\mu_1 + \frac{\mu_2 - \mu_1}{I_0/I + 1}\right] p_s. \tag{4.14}$$

For the wall frictional shear stress, Holyoake (2012) proposed $\frac{h}{w}$ as the relevant parameter to characterize the effect of the side wall on the flow, where h is the depth of the flowing layer, and w is the width of the screen. Similarly,

$$\tau_w = \mu_w \left(\frac{h}{w}\right) p_s \tag{4.15}$$

where μ_w is the frictional coefficient of the side walls.

Appropriately,

$$\tau_s = \left[\mu_1 + \frac{\mu_2 - \mu_1}{I_0/I + 1}\right] p_s + \mu_w \left(\frac{h}{w}\right) p_s \tag{4.16}$$

Using this representation, it is observed that as the flow accelerates, the friction decreases and hence the stress.

Jenkins and Richman (1985) developed a granular kinetic theory for three-dimensional spheres to model the kinetic stress in granular flow. This model has been validated both experimen-

tally and numerically. Using collisional arguments, Lee and Huang (2012) and Pathmathas (2015) expressed the region captured by the kinetic regime as:

$$\tau_c = k\rho_p(\lambda d)^2 \left(\frac{Du_1}{Dx_2}\right)^2 \tag{4.17}$$

where ρ_p, d, and λ are the material density, the grain diameter, and the linear grain density, respectively; $\frac{Du}{Dx_2}$ is the stress rate perpendicular to the depth of flow; and k is the proportionality constant which is approximately equal to 1. The linear grain density λ is expressed in terms of the radial distribution (g_0) (measure for the probability of inter-particle contact) and volume concentration (ϕ) as:

$$\lambda = g_0 - 1, \tag{4.18}$$

and

$$g_0 = \left[1 - \left(\frac{\phi}{\phi_c}\right)^{1/3}\right]^{-1} \tag{4.19}$$

where ϕ_c is the maximum particle packing (Bagnold 1954b; Savage and Hutter 1998).

The corresponding normal stress (p_c) is $\approx (1/3)\tau_c$ from the granular flow investigations of Bagnold (1954b), Armanini et al. (2005), and Roufail et al. (2012). p_c can therefore be expressed as:

$$p_c = \frac{1}{3}\rho_p(\lambda d)^2 \left(\frac{Du_1}{Dx_2}\right)^2 \tag{4.20}$$

To derive the turbulent stress, Prandtl's mixing theory which postulates that

$$\mathbf{u} \sim \ell \left|\frac{Du}{Dy}\right| \tag{4.21}$$

was applied, where $\mathbf{u}$ is the turbulent velocity and ℓ is the mixing length. From equation 4.17 Takahashi (2009) expressed turbulent stress as:

$$\tau_t = \rho\ell^2 \left(\frac{Du_1}{Dx_2}\right)^2 \tag{4.22}$$

where ρ is the bulk density of the granular particles, expressed as $\rho = \phi\rho_p$. Ashida et al. (1985) and Hotta (2012) define ℓ as:

$$\ell = k_t \rho d^2 \left(\frac{1-\phi}{\phi}\right)^{2/3} \tag{4.23}$$

k_t depends on the nature of the flow and space. In this work the value of k_t was obtained from simulation by choosing a mixing length of $\ell \sim 20d$ within the region of steady flow. The choice of ℓ is inspired by the findings of Hotta (2012) who worked on debris flow on an inclined channel. In his work, Hotta (2012) observed an excess pressure beyond the hydrostatic pressure as debris sediments increase along the channel. The increasing pressure is attributed to turbulence in the system and is expressed by equation 4.25. The choice of ℓ and the subsequent derivation of $k_t = 2.2$ is based on the results for steady flow from the base case simulation. Substituting ρ in equation 4.22, the turbulent shear stress is expressed as

$$\tau_t = k_t \rho_p d^2 \phi^{1/3} (1-\phi)^{2/3} \left(\frac{Du_1}{Dx_2}\right)^2 \tag{4.24}$$

In the turbulent regime, the expression for the normal turbulent stress p_t and the turbulent shear stress τ_t are identical according to Hotta (2012) i.e.

$$p_t = k_t \rho_p d^2 \phi^{1/3} (1-\phi)^{2/3} \left(\frac{Du_1}{Dx_2}\right)^2. \tag{4.25}$$

The normal stress in the static regime can be obtained by subtracting the turbulent normal stress and the kinetic-collisional normal stress from the total normal stress, i.e.

$$p_s = p - p_c - p_t \tag{4.26}$$

The total shear stress τ and the total pressure p are respectively obtained by adding their constituents as described above, i.e. (τ_s, τ_c, τ_t) and similarly (p_s, p_c, p_t).

Thus:

$$\tau = \mu_i(I) p_s + \mu_w \left(\frac{h}{w}\right) p_s + k\rho_p(\lambda d))^2 \dot{\gamma}^2 + \rho \ell^2 \dot{\gamma}^2 \tag{4.27}$$

where the shear rate $\dot{\gamma} = \frac{Du_1}{Dx_2}$.

By applying equations 4.26 and 4.27, the total stress τ can be expressed as

$$\tau = \left[\mu_i(I) + \mu_w \left(\frac{h}{w}\right)\right](p - p_c - p_t) + \rho_p(\lambda d)^2\dot{\gamma}^2 + k_t\rho d^2\phi^{\frac{1}{3}}(1-\phi)^{\frac{2}{3}}\dot{\gamma}^2 \tag{4.28}$$

Taking the ratio of the total shear stress τ and total pressure p gives the effective friction coefficient $\mu(I)$ for the vibrating screen flow. Thus:

$$\frac{\tau}{p} = \mu(I) = \left[\mu_i(I) + \mu_w \left(\frac{h}{w}\right)\right]\left[1 - \frac{3}{p}\rho_p(\lambda d)^2\dot{\gamma}^2 - \frac{1}{p}k_t\rho_p d^2\phi^{\frac{1}{3}}(1-\phi)^{\frac{2}{3}}\dot{\gamma}^2\right] + \frac{1}{p}\rho_m(\lambda d)^2\dot{\gamma}^2 + \frac{1}{p}k_t\rho_p d^2\phi^{\frac{1}{3}}(1-\phi)^{\frac{2}{3}}\dot{\gamma} \tag{4.29}$$

However, the model is difficult to use in this form; a further re-arrangement makes it easier to apply. Given that:

$$I^2 = \frac{\dot{\gamma}^2 d^2}{p/\rho_p}, \tag{4.30}$$

equation 4.29 can be expressed as:

$$\mu(I) = \left[\mu_i(I) + \mu_w \left(\frac{h}{w}\right)\right]\left[1 - 3\lambda^2 I^2 - k_t\phi\left(\frac{1-\phi}{\phi}\right)^{\frac{2}{3}} I^2\right] + \lambda^2 I^2 + k_t\phi\left(\frac{1-\phi}{\phi}\right)^{\frac{2}{3}} I^2. \tag{4.31}$$

To assess if the model can give the expected effective friction coefficient, the parameters in Table 4.1 (which were extracted from simulation results) were inserted into equation 4.31 to plot a graph of the variation of effective friction coefficient with inertial number:

Table 4.1: Average parameters for Figure 4.5

Parameter	Values	Description
l	$20d$	mixing length
d	0.004	average particle diameter
h	0.025	average bed depth
w	0.480	length of the screen
μ_1	$tan(20.9)$	Critical angle of steady flow
μ_2	$tan(32.8)$	Limiting angle of steady flow
μ_w	0.7	sidewall friction coefficient

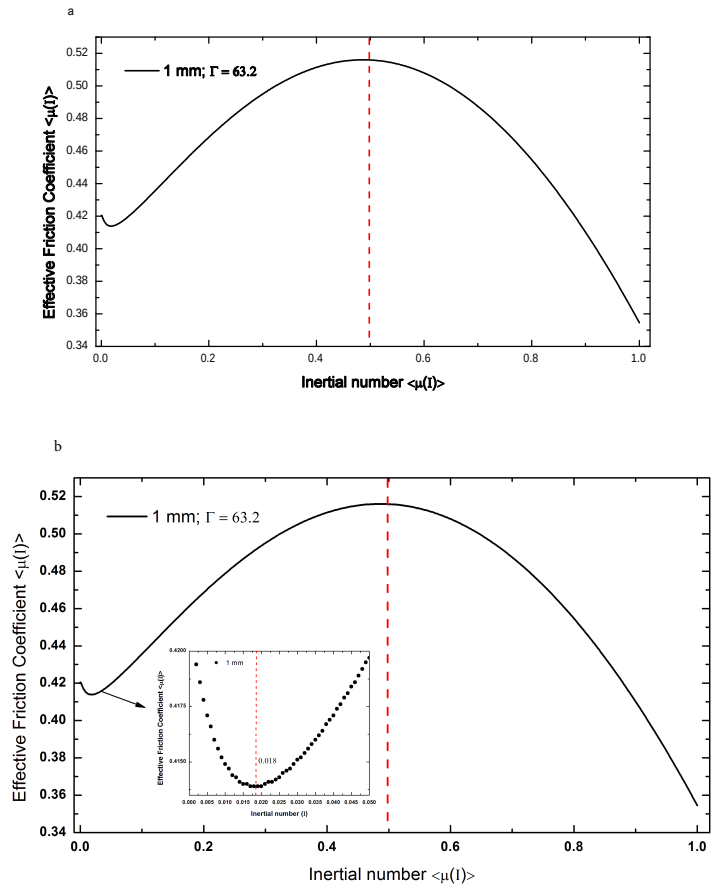

Figure 4.5: A plot of the variation of effective friction coefficient with inertial number using the base case of 1mm amplitude and 4Hz Frequency. The model is a plot of equation (4.32) using the average values from Table (4.1). The model captures the phase transitions from a quasi-static flow (where $I = 0.018$) to a dense liquid-like flow, and to a gas-like flow (where $I = 0.5$). The phase transitions are captured at inertial numbers that correspond to the solids concentration measurements for different regimes of flow. The inset on the left corner of the Figure 4.5 (b) shows the transition from the quasi-static flow.

The model described in Figure 4.5 captures the flow transition from a quasi-static phase to a

dense-flow regime. The inset in Figure 4.5 (b) shows the hysteresis effect and the transition to a dense-like regime. The value of I at the point of transition is 0.018 i.e. the quasi-static regime occurs at $I \leq 0.018$. The model also captures the transition from a dense-like regime to a turbulence or gas-like regime. This transition occurs at the value of $I = 0.5$ i.e. the dense flow regime occurs at $0.018 < I < 0.5$. Beyond the dense-flow regime is where the inertial regime occurs. As shown in Figure 4.3, the region close to the surface is where the transition to the inertial and the turbulent regime is experienced. This transition is the limitation that Lee and Huang (2012) suggested warranted further study (see section 2.6).

4.3 Summary

In order to understand the dynamics of particulate flow on an inclined vibrating screen, a constitutive stress model of granular flow on an inclined vibrating screen was developed in this chapter. Key parameters in the granular flow model (velocity, shear rate and volume fractions) were extracted from DEM simulations. The data were utilized to calculate the shear stress distribution from the developed model. An important dimensionless parameter that was used to determine the flow transition and the different regimes of flow is the inertial number. It was established that the variation of the effective friction coefficient with the inertial number controls the flow on the screen.

Chapter 5

Energy Dissipation, Results and Discussion

5.1 Introduction

The previous chapter reveals that granular flow on an inclined vibrating screen exhibits different flow regimes and that these regimes have been successfully captured by a rheological mesoscopic model. The model developed in Chapter 4 shows the transition from one regime to another and the variation of the effective friction coefficient with the inertial number I. In this chapter, the focus is on how this phenomenological model can be applied to screening. The screening application used here is limited to the bulk behaviour of particles on an inclined vibrating screen. The granular flow is a dry mixture of two particle constituents of diameters 3 mm and 5 mm. The aperture size is 3.5 mm square and the angle of inclination is set at $\theta = 25°$.

The base case condition discussed in Chapter 3 was employed for the analysis of the different flow regimes. Subsequently, the effect of the intensity of vibration on the flow regimes was examined by varying the amplitude and the frequency of vibration as stated on Table 3.1. The

transition from one regime to another in the case of an inclined vibrating screen is controlled by the inclination of the screen (θ), and the dimensionless acceleration Γ of the bed.

$$\Gamma = \frac{a\omega^2}{g} \tag{5.1}$$

where a is the amplitude of vibration, ω is the angular frequency and g is the acceleration due to gravity, and

$$\omega = 2\pi f \tag{5.2}$$

where f is the frequency of vibration. In this work, a sinusoidal vibration of the form:

$$y(t) = asin(\omega t) \tag{5.3}$$

was employed for the shaking of the screen, where $y(t)$ is the vertical displacement of the screen at time (t).

Under sufficient mechanical agitation or shear stress, granular media yield and flow occur. In this work, both mechanical agitation (in the form of vibration) and the inclination of the screen are responsible for the granular flow down the screen surface. The energy input by the sinusoidal vibration of the screen is not evenly distributed, hence the different regimes of flow. Naturally, the flow of particles itself can induce mechanical agitations (Longhi et al. 2002). This agitation in the absence of an external vibration can be attributed to shear-induced agitation. In an inclined vibrating screen, both stress and mechanical agitation play a crucial role. The angle of inclination (or declination) must not be too high, otherwise the screen becomes too steep, reducing the residence time of granules on the screen and the chances of undersized particles falling through the screening aperture. At the same time, if the mechanical agitation during screening is too high, particles will bounce off the screen. In this work, the mechanical agitation and the sheared-induced agitation were maintained at a level suitable for screening (Chen and Xin 2009).

5.2 Energy input and dissipation

The vibration of the screen is the main source of energy supply to the granular flow along the screen. Despite a constant supply of energy to the flowing granules, the high rate of energy dissipation in the system does not permit an even distribution of the energy. The energy at the base is transmitted directly to the particles and the influence of vibration is high, but as the impact wave travels through the flow depth, there is a significant dissipation of energy. The primary aim of introducing vibration into an inclined screen configuration is to ensure the repositioning of particles as they travel along the screen. When they are repositioned, the chances of undersize materials falling through will increase. Largely, their behaviour in response to vibration is governed by the following dimensionless parameters: the dimensionless acceleration Γ, the energy input parameter Ω, and the dissipative parameter Θ:

$$\Omega = \frac{a^2\omega^2}{gd} \tag{5.4}$$

$$\Theta = N_l(1-e) \tag{5.5}$$

where N_l is the number of particle layers and e is the normal coefficient of restitution.

Warr et al. (1995) developed a simple model by relating the energy input by a vibrating wall and the energy dissipation in collisions under gravity, isothermal condition and with mean velocity of all particles. Further, Luding, Herrmann and Blumen (1994) studied the energy input by a vibrating wall and the energy dissipation in relation to the coefficient of restitution. In relation to screening, the focus of this work is limited to the effect of the vibration on the different regimes of flow. It is observed that despite varying the intensity of vibration within a reasonable level applicable to screening, the energy input both by induced shear and the vibration of the screen are not evenly distributed. While some particles are almost static, some flow rapidly. Details of modelling the energy input by a vibrating wall can be found in Luding, Clément, Blumen, Rajchenbach and Duran (1994). The effects of the intensity of

vibration on the model developed in Chapter 4 will be discussed later in this chapter. From this investigation the dominant stress and the regime that is favourable for screening can be identified.

5.3 Analysis of different flow regimes

This work assumes that the energy dissipation through particle-particle collisions is responsible for the different regimes. These regimes are discussed in this section with respect to the base case of $f = 4\ Hz$ and $a = 1\ mm$. The model presented in Chapter 4 can be disintegrated into three flow constituent stresses and effective frictional regimes. This makes it possible to study the extent to which each constituent regime affects screening.

5.3.1 The quasi-static regime

In this work, despite the vibration of the geometry, results from simulation show a regime that is almost stationary. This regime is referred to in this work as the quasi-static regime. Many reasons could be responsible for this phenomenon, ranging from inter-locking of particles due to uneven distribution of the mechanical agitation to the upward and downward movement of the oversize and undersize particles (segregation). Further, some particles get stuck inside the aperture of the screening surface while the roughness of the surface caused by the screening aperture opposes the flow of particles (wall friction - as discussed in the previous chapter).

Intuitively, one would expect particles flowing on a vibrating surface to be fluidized but sometimes they bounce into each other and the frictional force between colliding particles tends to retard their free flow. This regime is dominated by friction and the mesoscopic analysis performed in this work captures a quasi-static regime. Figure 5.1 shows the variation of static pressure and shear stress at different scaled depths. The quasi-static regime dominates the region between scaled depth $0 - 0.5$. Beyond this depth, a transition to a dilute regime

occurs, as the quasi-static regime decreases towards the surface i.e. $\tau_s, p_s \to 0$. This further alludes to the observation from the graph of solids concentration versus scaled depth (Figure 4.3) that the solids concentration decreases towards the surface which implies a rapid flow.

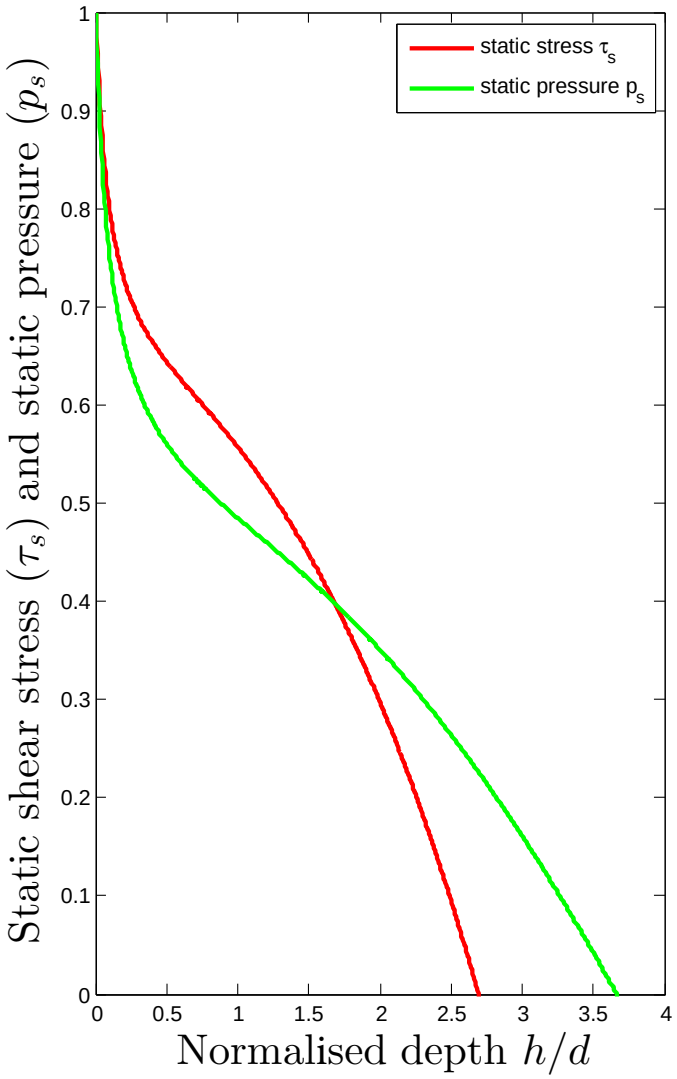

Figure 5.1: Variation of the static pressure and stress with the scaled depth of flow

At depth 0 in Figure 5.1 (which corresponds to point A in Figure 4.3), the volume fraction is high ($\phi = 0.58$) (readings are taken from this point to the surface 0-5) which confirms the presence of many particles. At this point, the particles are locked into stress chains, and interact with each other through persistent contacts. As particles gain the energy to break

the stress chain, a collisional regime gradually sets in. At depth 1.7, the stresses intersect confirming that, occasionally, a portion of the particle flow can be stationary. Moreover, as the depth increases towards the surface, both stresses reduce until they both vanish. The static shear stress is higher before the intersection because the tendency of particles to move toward the flowing direction is higher. However, the static pressure extends beyond the static stress because as long as particles exist on the screen, they will experience gravitational force acting parallel to the depth. The model developed in Chapter 4 captures the quasi-static regime and its gradual transition into a collisional regime (see the inset in Figure 4.5). The hysteresis effect and the transition from the quasi-static regime occurs at $I \leq 0.018$.

5.3.2 The kinetic regime

Figure 5.2 shows the variation of collisional pressure and shear stress with scaled depth of particle flow along the screen. It can be seen that at this sampling point, both the collisional shear stress and pressure increase sharply from the scaled depth of 0 to 1.0. The maximum value for τ_c is 0.33 and for p_c, 0.46. These values are within the quasi-static regime i.e. the dominant regime within this depth of flow is the quasi-static regime. In other words, despite the sharp increase in τ_c and p_c, $\tau_s > \tau_c$ and $p_s > p_c$ within this depth ($0 \leq h/d \leq 1.0$). A drop was noted in τ_c from scaled depth 0.68 to 2.7. likewise, a drop was noted in p_c from depth 1.1 to the surface at depth 4.6. The drop in both τ_c and p_c is due to the co-existence of both the static effect, resulting from enduring contact, and the kinetic effect, comprising both collision and inertial effects, in this region.

The kinetic regime in this work could otherwise be described as the dense, liquid-like regime where frictional and collisional effects are active. At the depth where $\tau_s \to 0$ ($h/d = 2.7$), τ_c begins to rise towards the surface (compare Figure 5.1 and Figure 5.2). The increase in the kinetic stress is not surprising, because towards the surface the particles move rapidly and contacts are by collisional effects. However, despite the co-existence of the static and the

kinetic effects, the kinetic regime is dominated by collisional-kinetic stress. This regime was captured by the model in Chapter 4 as the region corresponding to $0.018 < I < 0.5$.

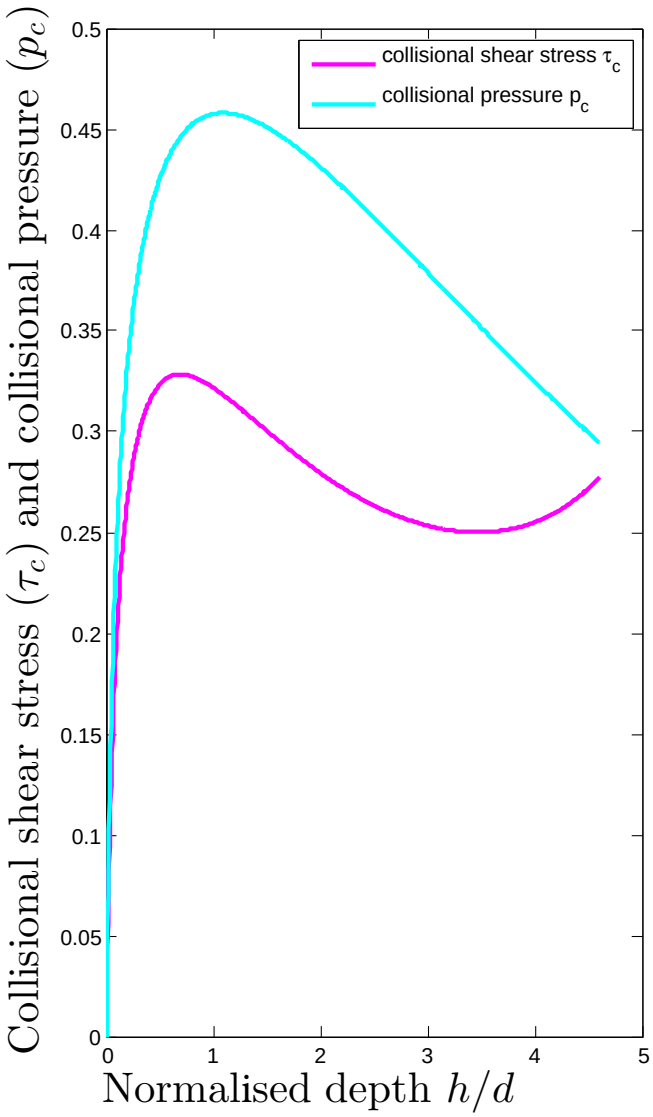

Figure 5.2: Variation of collisional pressure and stress with the scaled depth

5.3.3 The turbulent regime

The chaotic interactions of particles which lead to the bouncing of some particles off the screen surface facilitate the introduction of a turbulent regime. From the simulation video, a chaotic interaction was noted towards the surface, with some particles occasionally bouncing off the

surface of the screen. Figure 5.3 reveals the turbulence within the flow. It can be seen that between $0 \leq h/d \leq 1$, some degree of turbulence is observed ($\tau_t, p_t \approx 0.1$)albeit negligible. As discussed in sections 5.3.1 and 5.3.2, τ_s and p_s dominate the depth $0 \leq h/d \leq 1$, and hence the level of turbulence within this region is expected to be ≈ 0. Beyond depth $h/d = 1$, a sharp increase is noted in τ_t towards the surface of the flow while p_t increases as well, $\tau_t >> p_t$. Although some degree of turbulence is seen within the flow, the region closer to the surface and the surface are significantly affected. The normal turbulent stress (turbulent pressure) is expected to decrease towards the surface in an open surface flow because the chaotic flow at the surface is essentially caused by the turbulent shear stress τ_t.

The turbulent pressure (p_t) towards the surface depends on the gravitational force as the normal stress. Within the bulk of the flow, p_t is developed by interactions with particles in the normal direction. However, towards the surface there is no confinement since the system geometry is an open surface. Although the values of the turbulent pressure are low compared to the turbulent shear stress towards the surface, they are essential to determining the effective frictional co-efficient and the corresponding inertial value for the turbulent regime. The shear turbulent stress τ_t dominance at the surface is due to the bumpy flow experienced by some particles as a result of the agitation from the vibration of the screen. From Figure 5.3, both the turbulent shear stress and turbulent pressure can be expressed mathematically as an exponential functions of the form τ_t,

$$p_t = a_t \exp\left(b_t(\frac{h}{d})\right), \tag{5.6}$$

where a_t and b_t are constants whose values depend on the level of turbulence in the flow. The model in Chapter 4 successfully captures the transition to the gas-like regime which is dominated by both the inertial and the turbulence effects.

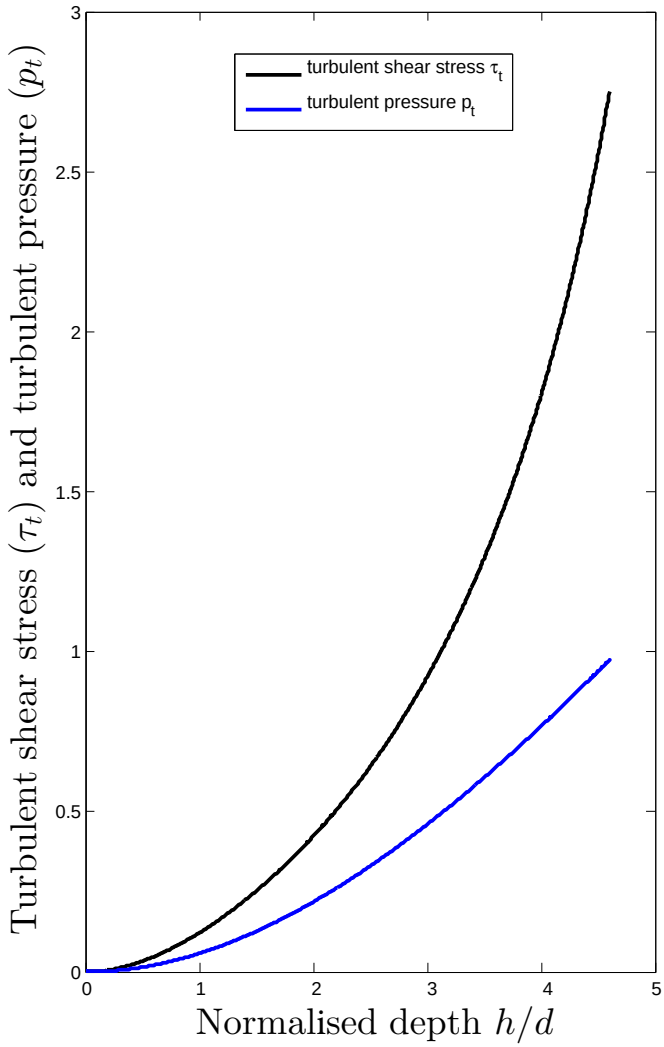

Figure 5.3: Variation of turbulent stress and pressure with the scaled depth

5.4 Velocity and fluctuation velocity

In Chapter 3, the continuum velocity field $\vec{u}^{\beta}$ is expressed as $\vec{u}^{\beta} = \frac{\vec{\vartheta}^{\beta}(\vec{r},t)}{\rho^{\beta}(\vec{r},t)}$ where $\vec{u}^{\beta}$ is the average velocity. The fluctuating part of the velocity of particle i (with respect to the coarse graining center r and time t) is

$$\vec{u}^{\beta}(r, tt') \equiv \vec{u}^{\beta}(t') - \vec{u}^{\beta}(r, t) \tag{5.7}$$

Figure 5.4 shows the variation of the velocity profile in the direction of flow with the scaled depth at steady state. Figure 5.4 (a) shows the velocity profile of each constituent particle (3 mm and 5 mm) and the average velocity of the flow. The average velocity in Figure 5.4 (b) was employed to describe the velocity of the flow in this work. As highlighted in the figure, the velocity is almost linear except for two zones within the dense liquid-like regime and towards the surface, where mechanical agitation causes a gas-like flow. Further, in Figure 5.4, the error bars denote the fluctuating parts of the velocity.

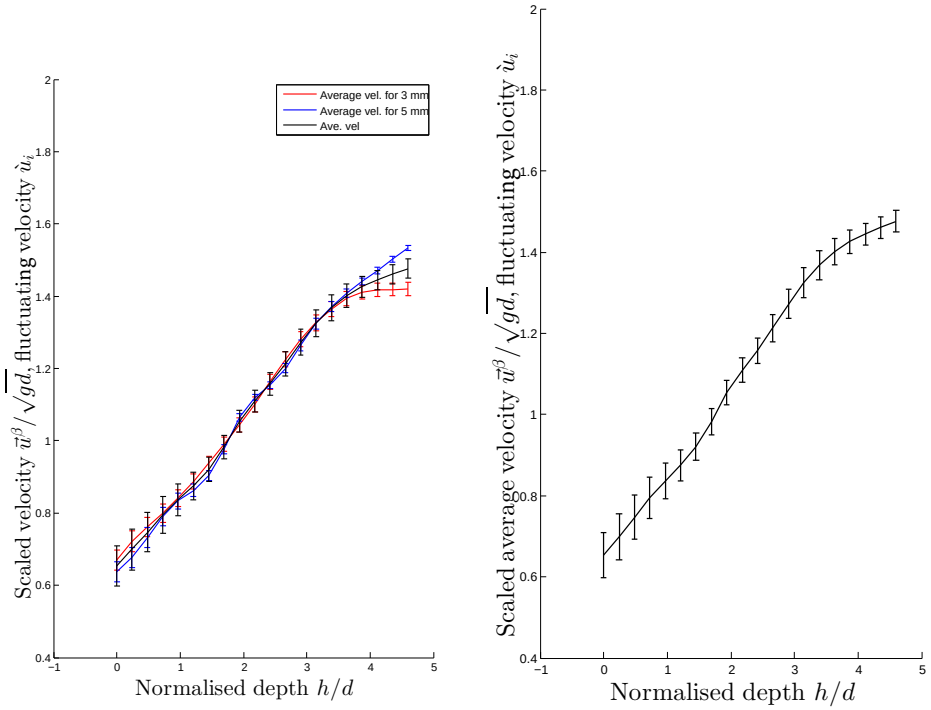

Figure 5.4: Variation of scaled velocity and fluctuating velocity with scaled depth

The fluctuating velocity $\grave{u}$ (discussed in section 4.2) can also be expressed as a function of the granular temperature T with respect to the mean velocity $\langle v \rangle$, i.e $\grave{u} = v - \langle v \rangle$ (Babic 1997). This implies further that the error bars in Figure 5.4 show the negligible thermal fluctuations in the system. As discussed earlier in section 4.2, the granular temperature T, which is analogous to the thermodynamic temperature, represents the energy associated with the random motion in the kinetic regime. This energy, however, dissipates within the granular flow along the screen. While the thermal fluctuation in the system is negligible, the results

(Figure 5.4) show a slight increase in thermal fluctuation close to the surface where the kinetic and turbulent regimes are prominent.

Further analysis of Figure 5.4 reveals that for oversize particles, at the depth where percolation of undersize particles occurs, the particles are more loose and collide rapidly with each other and with the walls of the geometry - hence, the higher fluctuation in the velocity of the oversize particles and the average velocity values close to the surface. Furthermore, close to the base where percolation of particles occurs and where the impact of vibrational energy is transmitted to the bulk of the flow, a slight increase in thermal fluctuation is noticed. Although the granular temperature $T = 1/3(\grave{u}_i^2)$, velocity fluctuation has been used in this work to describe the thermal fluctuation in the flow. The model in Chapter 4 was developed on the assumption of an athermal flow in the system of study. The reason for this assumption can be seen in the above analysis, where 1/3 of the fluctuating velocity ($\grave{u}$) is negligible.

5.5 Shear rate

In Figure 5.5 the shear rate delineates the three flow regimes. In the quasi-static regime, the shear rate increases linearly with depth until it reaches a point where $\dot{\gamma} = 10.99s^{-1}$. At this point, there is a transition to an intermediate regime where the volume fraction is relatively constant (Figure 5.5). Another transition occurs at $\dot{\gamma} = 14.76s^{-1}$, which corresponds to the depth where the inertial regime begins. The granular velocity perpendicular to the depth of flow at this point increases, and hence the change in the shear rate. The average shear rate value for the flow is $\approx 13s^{-1}$ at a constant fit value of $\dot{\gamma} \approx 1.7\left(\sqrt{\frac{g}{\langle d \rangle}}\right)$ using the same scaling magnitude as the results obtained in section 3.2.3.

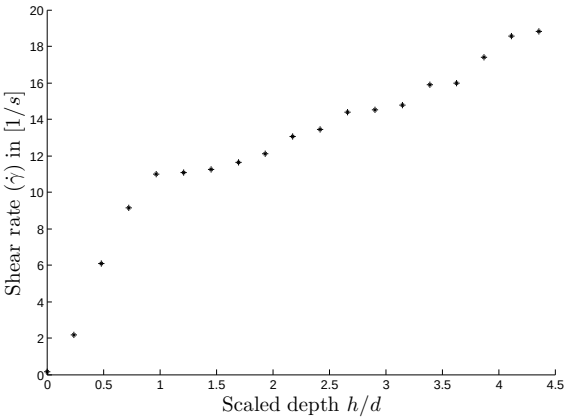

Figure 5.5: Variation of shear rate ($\dot{\gamma}$) with scaled depth

5.6 The effects of vibration intensity on the effective friction coefficient variation with the inertial number

In the model developed in Chapter 4, readings were taken from the simulation result of the base case where the frequency of vibration and amplitude were 4 Hz and 1 mm respectively. In Figure 5.6, the intensity of vibration is varied by increasing the frequency of vibration as shown in Table 3.1 while the amplitude is fixed at 1 mm. It can be seen that an increase in frequency affects essentially the static regime. The quasi-static regime vanishes as the frequency of vibration increases. The gradual disappearance of this regime shows the effect of vibration on the flow. Although the focus of this work is limited to granular flow on an inclined vibrating screen, much work has been done on the impact of vibration on the efficiency of a screen (Hilden 2007; Kelly and Spottiswood 1982; Williams 1963; 1976; Chen and Xin 2009): an increase in the frequency of vibration will increase the level of energy supply to the flow and consequently the chances of undersize particles falling through.

Ideally, the purpose of vibration in screening is to reposition particles in order to present them in the best position to penetrate the screening aperture. In this work, the effect of the increase in vibration suggests a regime that is dominated by kinetic and turbulent effects. At high vibration intensity, when the turbulent regime dominates the system, particles may

bounce off the screen which is not good for screening efficiency. In order to maintain a normal screening condition, frequency should be maintained at a level where turbulence is reduced significantly. The variation of the effective friction coefficient with the inertial number will help to monitor the flow regime. The transitions to different regimes occur at different inertial numbers. Further to this, the inertial number will help to determine the effects of different screening parameters on the flow. The vibration intensity Γ in Figure 5.6 was calculated from the increase in frequency. Similarly, Figure 5.7 shows the effect of an increase in amplitude on the flow regimes when the frequency of vibration was fixed at 4 Hz. A similar effect to the increase in frequency of vibration was observed but the figure shows that the model is more sensitive to changes in amplitude than changes in the frequency of vibration.

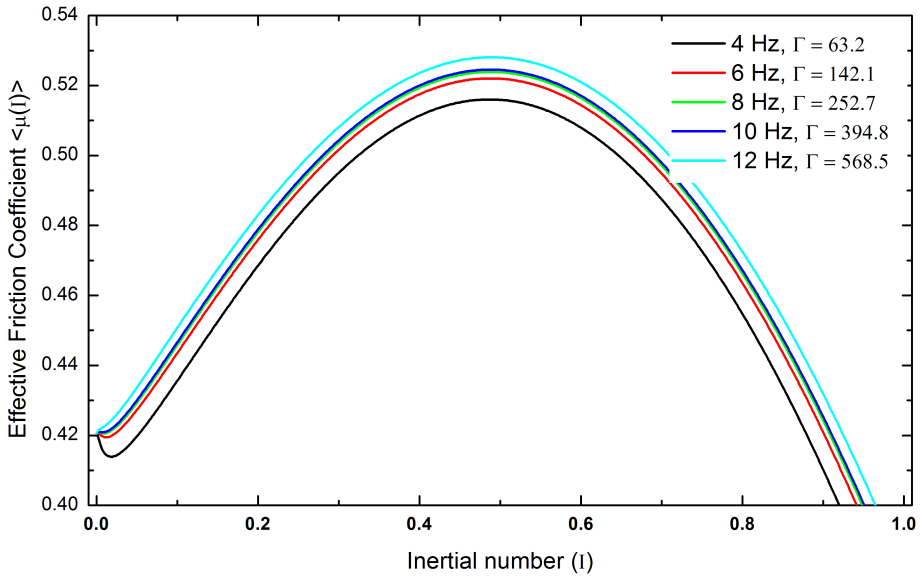

Figure 5.6: A plot of the variation of effective friction coefficient with inertial number at a fixed amplitude of 1 mm and different frequencies. The effects of the frequency of vibration on the flow are seen in the variation of the inertial number at transitions to different flow regimes (see details in Table 5.1)

.

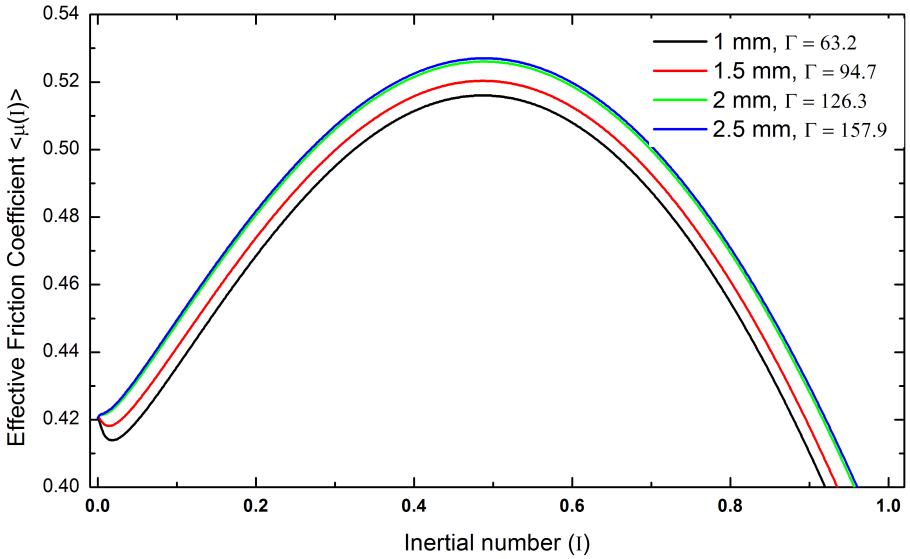

Figure 5.7: A plot of the variation of effective friction coefficient with inertial number at a fixed frequency of 4 Hz and different amplitudes. The effects of the amplitude of vibration on the flow are seen in the variation of the inertial number at transitions to different flow regimes (see details in Table 5.2)

Table 5.1: Inertial values for regimes transitions as frequency increases

Frequency (Hz)	Values of I at transition from a quasi-static regime to a dense liquid-like regime	Values of I at transition from a dense liquid-like regime to a turbulent regime
4	0.018	0.490
6	0.012	0.494
8	0.009	0.498
10	0.004	0.498
12	0	0.510

Table 5.2: Inertial values for regimes transitions as amplitude increases

Amplitude (mm)	Values of I at transition from a quasi-static regime to a dense liquid-like regime	Values of I at transition from a dense liquid-like regime to a turbulent regime
1.0	0.018	0.490
1.5	0.013	0.493
2.0	0.001	0.502
2.5	0	0.508

Chapter 6

Conclusions and Recommendations

After analysis of relevant literature on computational modelling of granular flow, this work applied the Discrete Element Methods (DEM) to study the rheological behaviour of granular flow on a vibrating screen. It was established that, if correctly implemented, DEM can accurately generate data for granular flow on an inclined vibrating screen. A review of different methods for modelling screening efficiency was discussed in this thesis; however, these models largely apply to the impact of the machine (screen) variables on the flow. To go beyond the current state-of-the-art in screen modelling, an understanding of the particle motion along an inclined vibrating screen is required. To this end, this work took the initiative to study the rheological behaviour of granular materials on vibrating inclined screens.

6.1 Conclusions

It is acknowledged that much study has been done to improve screening efficiency, but to the best knowledge of the author, little or no work has been done from a rheological perspective. A model of screening was developed in this work to model the mechanisms (not the machine) of granular flow on an inclined vibrating screen. DEM was employed to perform simulations for studying the granular flow of a mixture of 3 mm and 5 mm glass beads on an inclined

vibrating screen. The aperture size and the angle of inclination were fixed at 3.5 mm and 25^0, respectively. The frequency and the amplitude of vibration were fixed at 4 Hz and 1 mm, respectively for the base case used to study the rheological behaviour. Subsequently, the intensity of vibration (comprising the frequency and amplitude) was varied to see the effects on the dynamics of the flow.

A micro-macro transition method in the form of the coarse-graining method of Tunuguntla (2015) was employed in this work. It was applied both to calibrate and validate continuum models from discrete data obtained from DEM simulations. The information extracted from discrete particle simulations was used both to confirm the assumptions of and provide the required closure rules for a rheological model that characterises the granular flow on an inclined vibrating screen. While microscopic properties were employed for the simulation, the properties extracted from the simulation are macroscopic fields which are consistent with the continuum equations of mass, momentum, and energy balance.

From the continuum equations, the volume fraction and the tangential velocity were determined as a function of the depth of flow. Data were extracted when the system attained a steady flow. The velocity and volume fraction distribution delineate different flow regimes in the flow. These flow regimes make it difficult to obtain a clear constitutive choice for the shear stress. By fitting the average scaled flow rate and the tangential velocity data to the normalised depth, scaling relation of the form $\left[\sqrt{Q^*} \propto (h/d)^n\right]$, where $n = 0.239 \pm 0.03$, and $\left[\langle V \rangle \propto (h/d)^n\right]$, where $n = 0.4017 \pm 0.03$, were obtained for the flow rate and velocity respectively. These values were the closest when compared to similar results in the literature (Bagnold 1954b; MiDi 2004; Jop et al. 2006; Felix et al. 2007).

Similar to the Bagnold profile, a relationship occur between the average velocity and the depth of flow ($\langle V \rangle \propto (h/d)^n$). For this profile, the scaling relation of $n = 0.4$ was observed which is used in place of Bagnoldian $n = 3/2$ for inclined plane geometry in Bagnold (1954b)

and Jop et al. (2006). This variance is associated with inclined vibrating screen geometry in which granular flow is influenced by the intensity of vibration, segregation and the percolation of particles. Further, under a linear scaling condition, the associated average shear rate is given by $\dot{\gamma}$ at constant fit of $\approx 1.7\left(\sqrt{\frac{g}{\langle d \rangle}}\right)$.

A constitutive stress model of granular flow on an inclined vibrating screen was developed which provide key mechanism of the dynamics of particle flow on an inclined vibrating screen. Key parameters to the granular flow model(velocity, shear rate and volume fractions) were extracted from DEM simulations. The data were utilized to calculate the shear stress distribution from the developed model. An important dimensionless parameter that was used to determine the flow transition and the different regimes of flow is the inertial number. It was established that the variation of the effective friction coefficient with the inertial number controls the flow on the screen. A critical examination of the volume concentration revealed the existence of the following:

(i) A static and quasi-static regime dominated by frictional stress, where $\phi = 0.58$.

(ii) A dense (liquid-like regime), where $0.4 < \phi < 0.58$. This regime allows both frictional and collisional-type stresses.

(iii) An inertial and turbulent regime, where $\phi < 0.4$. This regime has negligible stress chain and it is dominated by a chaotic flow. The introduction of a turbulent regime was informed by the chaotic behaviour at the surface of the screen. This turbulence was pronounced whenever the frequency of vibration was increased.

This work investigated the most appropriate relationship between the solids concentration (ϕ) and the inertial number (I) by comparing results from similar studies on open surface flow. The most appropriate relationship that describes the flow on an inclined vibrating screen was $\phi(I) = \phi_{max} \exp -bI^c$. The values of b and c that captured the flow were found to be 1.84 and 0.60, respectively. Subsequently, an effective frictional coefficient model that is based on frictional, collisional-kinetic and turbulent stress was developed in this work. This model

captured the following:

(i) The inertial frictional stresses (local rheology)in the densely flowing regions cf.Jop et al. (2006)

(ii) The kinetic-collisional stresses of Bagnold (1954b) in the dense regime, and

(iii) The inertial regime dominated by turbulent stress. The turbulent stress is supported by Hotta (2012), Suzuki et al. (2003), Ashida et al. (1985) and Pathmathas (2015).

The main stresses observed in the flow and the transitions between the flow regimes were successfully captured by this model. Of note is the transition beyond the dense-flow regime and the inertial regime which Lee and Huang (2012) suggested warranted further study.

In applying the granular flow model to screening, similar conditions to those which Chen and Xin (2009) suggested were appropriate for efficient screening were employed for the simulations in this work. The intensity of vibration was varied to see the effects on granular dynamics on the vibrating screen. It was observed that the model was sensitive to variations in the vibration intensity parameters. It was observed that increasing the vibration intensity could lead to the disappearance of the quasi-static regime and increase the turbulence in the system. The inertial values at which transitions occur are $I = 0.018$ and $I = 0.5$, respectively for the transitions to the kinetic and to the inertial regimes in the base case (where frequency is 4 Hz and amplitude is 1 mm). The values of I at which transitions occur varied in response to the variation of the vibration intensity. At high vibration intensity, the value of $I \to 0$ for the transition to the kinetic regime (since the quasi-static regime disappeared at this point). On the other hand, the values of I increases as the flow becomes fluidized (Table 5.1 and 5.2). The inertial values at which transitions occur can be recorded and used to monitor the flow.

The work described in this thesis is confined to developing a granular flow model for an inclined vibrating screen. In developing the model, this work established the dominant stress on the screen determines the dominant regime and hence the granular behaviour on the screen.

Further, the dynamics of the granular materials can be controlled by means of the model relating the variation of the effective frictional coefficient with the inertial number.

6.2 Recommendations and future work

A model for for an inclined vibrating screen was developed using a granular flow approach specifying granular flow in the system. However, further work is required to:

(i) Increase the particle fraction that can be considered so that interactions of the range of particles in the screen feed can be determined

(ii) The work was limited to a 2-dimensional flow behaviour, a fully 3-dimensional model utilizing a full tensorial formulation of granular flow via DEM simulation should be explored.

This work has taken the initiative to study granular flow on an inclined vibrating screen, future work should extend the phenomenological model developed in this work to calculating screening efficiency. To successfully integrate this model into calculating screening efficiency, a wide range of data (both discrete and empirical) must be tested to validate the model further. The impact of the DEM data on particle stratification and the screen performance, and how the model affects the performance of screens should also be investigated. Finally, the discrete micro-scale information from DEM needs to be recast into the continuum descriptions of the full stress tensor. The continuum schemes described by Goldhirsch (2003) will be useful to achieve this. A full tensorial formulation will interrogate the validity of the constitutive relations developed in this work.

Bibliography

Abdel-Aziz, Y.: 1971, Karara. hm (1971) Direct linear transformation from comparator coordinates into object-space coordinates in close-range photogrammetry, *Proceedings ASP/VI Symp. On Close-Range Photogrammetry*, pp. 1–17.

Ahmad, K. and Smalley, I.: 1973, Observation of particle segregation in vibrated granular systems, *Powder Technology* **8**(1), 69–75.

Alkhaldi, H. and Eberhard, P.: 2007, Particle screening phenomena in an oblique multi-level tumbling reservoir: a numerical study using discrete element simulation, *Granular Matter* **9**(6), 415–429.

Allen, T.: 2013, *Particle size measurement*, Springer London.

Ancey, C.: 2002, Dry granular flows down an inclined channel: Experimental investigations on the frictional-collisional regime, *physical review-series E-* **65**(1; PART 1), 011304–011304.

Ancey, C., Coussot, P. and Evesque, P.: 1999, A theoretical framework for very concentrated granular suspensions in a steady simple shear flow., *J. Rheol* **43**, 1673–1699.

Andreotti, B., Forterre, Y. and Pouliquen, O.: 2013, *Granular media: Between Fluid and Solid*, Cambridge University Press. Cambridge. U.K.

Apling, A.: 1984, Blinding of screens by sub-sieve sized particles, *Transactions of the Institution of Mining and Metallurgy. Section B. Applied earth science* **93**, C92–C94.

Armanini, A., Capart, H., Fraccarollo, L. and Larcher, M.: 2005, Rheological stratification

in experimental free-surface flows of granular-liquid mixtures, *Journal of Fluid Mechanics* **532**, 269–319.

Ashida, K., Egashira, S., Kamiya, H. and Sasaki, H.: 1985, The friction law and moving velocity of a soil block on slopes, *Technical report*, Kyoto University.

Azanza, E., Chevoir, F. and Moucheront, P.: 1999, Experimental study of collisional granular flows down an inclined plane, *Journal of Fluid Mechanics* **400**, 199–227.

Babic, M.: 1997, Average balance equations for granular materials, *Int. J. Eng. Sci.* **35**, 523–548.

Bagnold, R. A.: 1954a, Experiments on a gravity-free dispersion of large solid spheres in a newtonian fluid under shear, *Proceedings of the Royal Society of London A: Mathematical, Physical and Engineering Sciences*, Vol. 225, The Royal Society, pp. 49–63.

Bagnold, R. A.: 1954b, Experiments on a Gravity-Free Dispersion of Large Solid Spheres in a Newtonian Fluid under Shear, *Proceedings of the American Royal Society of London. Series A, Mathematical and Physical Sciences* **225**, 49–63.

Batterham, R., Weller, K., Norgate, T. and Birkett, C.: 1980, Screen performance and modelling with special reference to iron ore crushing plants, *European Symposium on Particle Technology. European Federation of Chemical Engineering, Amsterdam, Netherlands*, pp. 1–16.

Bbosa, L. S.: 2013, *Probability based models for the power draw and energy spectra of a tumbling mill*, PhD thesis, University of Cape Town, South Africa.

Berton, G., Delannay, R., Richard, P., Taberlet, N. and Valance, A.: 2003, Two-dimensional inclined chute flows: Transverse motion and segregation, *Physical Review E* **68**(5), 051303.

Campbell, C. S.: 2002, Granular shear flows at the elastic limit, *Journal of Fluid Mechanics* **465**, 261–291.

Chen, Y.-h. and Xin, T.: 2009, Application of the dem to screening process: a 3d simulation, *Mining Science and Technology (China)* **19**(4), 493–497.

Chen, Y.-S., Hsiau, S.-S., Lee, H.-Y., Chyou, Y.-P. and Hsu, C.-J.: 2010, Size separation of particulates in a trommel screen system, *Chemical Engineering and Processing: Process Intensification* **49**(11), 1214–1221.

Ciamarra, M. P., Vizia, M., Fierro, A., Tarzia, M., Coniglio, A. and Nicodemi, M.: 2006, Granular species segregation under vertical tapping: Effects of size, density, friction, and shaking amplitude, *Physical review letters* **96**(5), 058001.

Cleary, P. W.: 2004, Large scale industrial dem modelling, *Engineering Computations* **21**(2/3/4), 169–204.

Cleary, P. W. and Sawley, M. L.: 2002, Dem modelling of industrial granular flows: 3d case studies and the effect of particle shape on hopper discharge, *Applied Mathematical Modelling* **26**(2), 89–111.

Clement, E. and Rajchenbach, J.: 1991, Fluidization of a bidimensional powder, *EPL (Europhysics Letters)* **16**(2), 133.

Clément, E., Vanel, L., Rajchenbach, J. and Duran, J.: 1996, Pattern formation in a vibrated two-dimensional granular layer, *Physical Review E* **53**(3), 2972.

Cross, M. C. and Hohenberg, P. C.: 1993, Pattern formation outside of equilibrium, *Reviews of modern physics* **65**(3), 851.

Cundall, P. A. and Strack, O. D. L.: 1979, A discreate numerical model for granular assemblies, *Geotechnique* **29**, 47–65.

Da Cruz, F., Chevoir, F., Roux, J. and Iordanoff, I.: 2003, Macroscopic friction of dry granular materials, *Tribology series* **43**, 53–61.

Da Cruz, F., Emam, S., Prochnow, M., Roux, J.-N. and Chevoir, F.: 2005, Rheophysics of dense granular materials: Discrete simulation of plane shear flows, *Physical Review E* **72**(2), 021309.

Daerr, A. and Douady, S.: 1999, Sensitivity of granular surface flows to preparation, *EPL (Europhysics Letters)* **47**(3), 324.

D'anna, G., Mayor, P., Barrat, A., Loreto, V. and Nori, F.: 2003, Observing brownian motion in vibration-fluidized granular matter, *Nature* **424**(6951), 909–912.

De Silva, S. R., Dyrøy, A. and Enstad, G. G.: 2000, Segregation mechanisms and their quantification using segregation testers, *IUTAM Symposium on Segregation in Granular Flows*, Springer, pp. 11–29.

Dehghani, A., Monhemius, A. and Gochin, R.: 2002, Evaluating the nakajima et al. model for rectangular-aperture screens, *Minerals Engineering* **15**(12), 1089–1094.

DEM-Solutions: 2006, *EDEM 2.4 User Guide*, 2005-2006 edn, DEM Solutions.

Di Renzo, A. and Di Maio, F. P.: 2004, Comparison of contact-force models for the simulation of collisions in dem-based granular flow codes, *Chemical Engineering Science* **59**(3), 525–541.

Di Renzo, A. and Di Maio, F. P.: 2005, An improved integral non-linear model for the contact of particles in distinct element simulations, *Chemical engineering science* **60**(5), 1303–1312.

Djordjevic, N.: 2003a, Discrete element modelling of power draw of tumbling mills, *Mineral Processing and Extractive Metallurgy* **112**(2), 109–114.

Djordjevic, N.: 2003b, Discrete element modelling of the influence of lifters on power draw of tumbling mills, *Minerals Engineering* **16**(4), 331–336.

Dong, K., Yu, A. and Brake, I.: 2009, Dem simulation of particle flow on a multi-deck banana screen, *Minerals Engineering* **22**(11), 910–920.

Douady, S., Fauve, S. and Laroche, C.: 1989, Subharmonic instabilities and defects in a granular layer under vertical vibrations, *EPL (Europhysics Letters)* **8**(7), 621.

El Khatib, W.: 2013, *Boundary Conditions for Granular Flows at Penetrable Vibrating Surfaces–Applications to Inclined Flows of Monosized Assemblies and to Sieving of Binary Mixtures*, PhD thesis, Worcester Polytechnic Institute.

Eshuis, P., van der Weele, K., van der Meer, D. and Lohse, D.: 2005, Granular leiden-

frost effect: experiment and theory of floating particle clusters, *Physical review letters* **95**(25), 258001.

Faiman, M. D. and Rippie, E. G.: 1965, Segregation kinetics of particulate solids systems iii. dependence on agitation intensity, *Journal of pharmaceutical sciences* **54**(5), 719–722.

Fan, Y., Schlick, C. P., Umbanhowar, P. B., Ottino, J. M. and Lueptow, R. M.: 2014, Modelling size segregation of granular materials: the roles of segregation, advection and diffusion, *Journal of Fluid Mechanics* **741**, 252–279.

Faraday, M.: 1831, On a peculiar class of acoustical figures; and on certain forms assumed by groups of particles upon vibrating elastic surfaces, *Philosophical transactions of the Royal Society of London* **121**, 299–340.

Felix, G., Falk, V. and D'Ortano, U.: 2007, Granular flows in a rotating drum: the scaling law between velocity and thickness of the flow, *Eur. Phys. J. E* **22**, 25–31.

Ferrara, G. and Preti, U.: 1975, A contribution to screening kinetics, *Proc. 11th Int. Miner. Proc. Congr., Cagliari* pp. 183–217.

Ferrara, G., Preti, U. and Schena, G.: 1988, Modelling of screening operations, *International Journal of Mineral Processing* **22**(1), 193–222.

Ford, K. J., Gilchrist, J. F. and Caram, H. S.: 2008, Density measurements in a vibro-fluidized deep granular bed, *The 2008 Annual Meeting*.

Forterre, Y. and Pouliquen, O.: 2002, Stability analysis of rapid granular chute flows: formation of longitudinal vortices, *Journal of Fluid Mechanics* **467**, 361–387.

Forterre, Y. and Pouliquen, O.: 2008, Flows of dense granular media, *Annu. Rev. Fluid Mech.* **40**, 1–24.

Gaudin, A. M., Gaudin, A. M., Gaudin, A. M., Minéralogiste, F., Gaudin, A. M. and Mineralogist, F.: 1939, *Industrial screening, in Principles of mineral dressing: Chapter 7*, Vol. 351, McGraw-Hill New York.

Gilardi, G. and Sharf, I.: 2002, Literature survey of contact dynamics modelling, *Mechanism and machine theory* **37**(10), 1213–1239.

Glasser, B. and Goldhirsch, I.: 2001, Scale dependence, correlations, and fluctuations of stresses in rapid granular flows, *Physics of Fluids (1994-present)* **13**(2), 407–420.

Goldhirsch, I.: 2003, Rapid granular flows, *Annual review of fluid mechanics* **35**(1), 267–293.

Goldhirsch, I.: 2010, Stress, stress asymmetry and couple stress: from discrete particles to continuous fields, *Granular Matter* **12**(3), 239–252.

Govender, I., McBride, A. and Powell, M.: 2004, Improved experimental tracking techniques for validating discrete element method simulations of tumbling mills, *Experimental Mechanics* **6**, 593–607.

Grozubinsky, V., Sultanovitch, E. and Lin, I. J.: 1998, Efficiency of solid particle screening as a function of screen slot size, particle size, and duration of screening the theoretical approach, *International journal of mineral processing* **52**(4), 261–272.

Hatano, T.: 2007, Power-law friction in closely packed granular materials, *Phys. Rev. E* **75**, 060301.
URL: *http://link.aps.org/doi/10.1103/PhysRevE.75.060301*

Hertz, H.: 1886, On the contact of rigid elastic bodies and on hardness, miscellaneous papers.

Hess, F. W.: 1983, Mathematical modelling of screens and related units for plant simulation.

Hilden, M. M.: 2007, *Dimensional analysis approach to the scale-up and modelling of industrial screens*, Phd thesis, University of Queensland, Australia.

Holyoake, A. J.: 2012, *Rapid granular flows in an inclined chute*, PhD thesis, University of Cambridge, U.K.

Hotta, N.: 2012, Basal interstitial water pressure in laboratory debris flows over a rigid bed in an open channel, *Nat. Hazards Earth Syst* **12**, 2499–2505.

Hsiau, S.-S. and Wang, J.-I.: 1999, Segregation processes of a binary granular mixture in a shaker, *Advanced Powder Technology* **10**(3), 245–253.

Huerta, D. and Ruiz-Suárez, J.: 2004, Vibration-induced granular segregation: a phenomenon driven by three mechanisms, *Physical Review Letters* **92**(11), 114301.

Hunt, K. and Crossley, F.: 1975, Coefficient of restitution interpreted as damping in vibroimpact, *Journal of applied mechanics* **42**(2), 440–445.

Iordanoff, I. and Khonsari, M.: 2004, Granular lubrication: toward an understanding of the transition between kinetic and quasi-fluid regime, *Journal of Tribology* **126**(1), 137–145.
URL: *http://dx.doi.org/10.1115/1.1633575*

Jenkins, J. and Richman, M.: 1985, Grad's 13-moment system for a dense gas of inelastic spheres, *Archive for Rational Mechanics and Analysis* **87**(4), 355–377.
URL: *http://dx.doi.org/10.1007/BF00250919*

Jenkins, J. T. and Savage, S. B.: 1983, A Theory for the Rapid Flow of Identical, Smooth, Nearly Elastic, Spherical Particles, *Journal of Fluid Mechanics* **130**, 187–202.

Jha, A. K. and Puri, V. M.: 2009, Percolation segregation of binary mixtures under periodic movement, *Powder Technology* **195**(2), 73–82.

Jop, P., Forterre, Y. and Pouliquen, O.: 2005, Crucial role of sidewalls in granular surface flows: consequences for the rheology, *Journal of Fluid Mechanics* **541**, 167–192.

Jop, P., Forterre, Y. and Pouliquen, O.: 2006, A constitutive law for dense granular flows, *Nature* **441**(7094), 727–730.

Josserand, C., Lagree, P. and Lhuillier, D.: 2006, Granular pressure and the thickness of a layer jamming on a rough incline, *Europhysics Letters* **73**, 363–369.

Karra, V.: 1979, Development of a model for predicting the screening performance of a vibrating screen, *CIM Bulletin* **72**(804), 167–71.

Kaye, B. and Robb, N.: 1979, An algorithm for deducing an effective sieve residue from the rate of powder passage through a sieve, *Powder Technology* **24**(2), 125–128.

Kelly, E. G. and Spottiswood, D. J.: 1982, *Screening and sieving, in Introduction to mineral processing: Chapter 9*, Wiley New York.

King, R. P.: 2001, *Size classification, in Modeling and simulation of mineral processing systems: Chapter 4*, Elsevier.

Kruggel-Emden, H. and Elskamp, F.: 2014, Modeling of screening processes with the discrete element method involving non-spherical particles, *Chemical Engineering & Technology* **37**(5), 847–856.

Lee, C.-H. and Huang, C.-J.: 2012, Kinetic-theory-based model of dense granular flows down inclined planes, *Physics of Fluids (1994-present)* **24**(7), 073303.
URL: *http://scitation.aip.org/content/aip/journal/pof2/24/7/10.1063/1.4736738*

Leonard, J. and Hardinge, B. C.: 1991, Coal preparation, society for mining, metallurgy, and exploration sme, *Inc. Littleton, Colorado* pp. 467–470.

Li, J., Webb, C., Pandiella, S. and Campbell, G. M.: 2002, A numerical simulation of separation of crop seeds by screening - effect of particle bed depth, *Food and bioproducts processing* **80**(2), 109–117.

Li, J., Webb, C., Pandiella, S. and Campbell, G. M.: 2003, Discrete particle motion on sieves - a numerical study using the dem simulation, *Powder Technology* **133**(1), 190–202.

Li, Z., Tong, X., Zhou, B. and Wang, X.: 2015, Modeling and parameter optimization for the design of vibrating screens, *Minerals Engineering* **83**, 149–155.

Liu, K.: 2009, Some factors affecting sieving performance and efficiency, *Powder Technology* **193**(2), 208–213.

Lois, G., Lemaitre, A. and Carlson, J.: 2006, Emergence of multi-contact interactions in contact dynamics simulations of granular shear flows, *EPL (Europhysics Letters)* **76**(2), 318.

Longhi, E., Easwar, N. and Menon, N.: 2002, Large force fluctuations in a flowing granular medium, *Physical review letters* **89**(4), 045501.

Luding, S. and Alonso-Marroquín, F.: 2011, The critical-state yield stress (termination locus) of adhesive powders from a single numerical experiment, *Granular Matter* **13**(2), 109–119.

Luding, S., Clément, E., Blumen, A., Rajchenbach, J. and Duran, J.: 1994, Onset of convection in molecular dynamics simulations of grains, *Physical Review E* **50**(3), R1762.

Luding, S., Herrmann, H. and Blumen, A.: 1994, Simulations of two-dimensional arrays of beads under external vibrations: Scaling behavior, *Physical Review E* **50**(4), 3100.

Lun, C., Savage, S., Jeffrey, D. and Chpeurniy, N.: 1984, Kinetic theory for granular flow: inelastic particles in couette flow and slightly inelastic particles in a general flow field, *Journal of Fluid Mechanics* **140**, 223–256.

Mainza, A., Evertsson, M., Benzer, H., Tavarese, M., Powell, M., Rule, C., Plint, N., Lombard, M. and Knopjes, B.: 2013, The role of classification in an evolving comminution circuit, *ESCC2013: 13th European Symposium on Comminution and Classification*, Sierke Verlag, pp. 67–71.

Mainza, A., Powell, M. and Knopjes, B.: 2004, Differential classification of dense material in a three-product cyclone, *Minerals Engineering* **17**(5), 573–579.

Makinde, O., Ramatsetse, B. and Mpofu, K.: 2015, Review of vibrating screen development trends: Linking the past and the future in mining machinery industries, *International Journal of Mineral Processing* **145**, 17–22.

Meinel, A.: 1998, Classification of fine, medium-sized and coarse particles on shaking screens, *AUFBEREITUNGSTECHNIK* **39**, 317–327.

Melo, F., Umbanhowar, P. and Swinney, H. L.: 1994, Transition to parametric wave patterns in a vertically oscillated granular layer, *Physical review letters* **72**(1), 172.

MiDi, G.: 2004, On dense granular flows, *The European Physical Journal E* **14**(4), 341–365.

Mindlin, R. D. and Deresiewica, H.: 1953, Elastic spheres in contact under varying oblique forces, *Journal of applied mechanics* **20**.

Miwa, S.: 1960, Proposal of a new index for expressing the performance of screens, *Kagaku Kogaku* **24**, 150–155.

Moon, B. Y., Kim, K. H., Kwak, K. H., Kang, G. J. and Hong, C. H.: 2008, Dynamic analysis and design of separation screen mechanism in a plant of moisturized wastes, *International Journal of Modern Physics B* **22**(09n11), 1449–1454.

Moon, S. J., Shattuck, M., Bizon, C., Goldman, D. I., Swift, J. and Swinney, H. L.: 2001, Phase bubbles and spatiotemporal chaos in granular patterns, *Physical Review E* **65**(1), 011301.

Mular, A. L. and Bhappu, R. B.: 1978, *Mineral processing plant design*, Society of Mining Engineers of the American Institute of Mining, Metallurgical, and Petroleum Engineers, Littleton Colorado.

Nedderman, R. M.: 2005, *Statics and kinematics of granular materials*, Cambridge University Press.

Olsen, J. L. and Rippie, E. G.: 1964, Segregation kinetics of particulate solids systems i. influence of particle size and particle size distribution, *Journal of pharmaceutical sciences* **53**(2), 147–150.

Orpe, A. V. and Khakhar, D.: 2001, Scaling relations for granular flow in quasi-two-dimensional rotating cylinders, *Physical review E* **64**(3), 031302.

Orpe, A. V. and Khakhar, D. V. V.: 2007, Rheology of surface granular flows, *Journal of Fluid Mechanics* **571**, 1–32.

Parker, D., Dijkstra, A., Martin, T. and Seville, J.: 1997, Positron emission particle tracking studies of spherical particle motion in rotating drums, *Chemical Engineering Science* **52**(13), 2011–2022.

Pathmathas, T.: 2015, *Granular flow modelling of rotating drum flows using positron emission particle tracking*, PhD thesis, University of Cape Town.

Peng, B.: 2014, *Discrete Element Method (DEM) Contact Models Applied to Pavement Simulation*, PhD thesis, Virginia Tech.

Pignatel, F., Asselin, C., Krieger, L., Christov, I. C., Ottino, J. M. and Lueptow, R. M.: 2012, Parameters and scalings for dry and immersed granular flowing layers in rotating tumblers, *Physical Review E* **86**(1), 011304.

Pouliquen, O.: 1999a, Scaling laws in granular flows down rough inclined plane, *Physics of Fluids* **11(3)**, 542–548.

Pouliquen, O.: 1999b, Scaling laws in granular flows down rough inclined planes, *Physics of Fluids (1994-present)* **11**(3), 542–548.

Pouliquen, O., Cassar, C., Jop, P.and Forterre, Y. and Nicolas, T.: 2006, Flow of dense granular material: Towards a simple constitutive laws, *Journal of Statistical Mechanics* **2006**, 7–20.

Pouliquen, O. and Chevoir, F.: 2002, Dense flows of dry granular material, *Comptes Rendus Physique* **3**(2), 163–175.

Prescott, J. K. and Carson, J. W.: 2000, Analyzing and overcoming industrial blending and segregation problems, *IUTAM Symposium on Segregation in Granular Flows*, Springer, pp. 89–101.

Rajchenbach, J.: 2003, Dense, rapid flows of inelastic grains under gravity, *Physical Review Letters* **90(14)**, 144302.

Roberto, D. P.: 1992, *Mathematical modelling of vibrating screens for plant simulation*, Master's thesis, University of The Witwatersrand, 1992. Typescript (Photocopy).

Rosato, A. D., Blackmore, D. L., Zhang, N. and Lan, Y.: 2002, A perspective on vibration-induced size segregation of granular materials, *Chemical Engineering Science* **57**(2), 265–275.

Rosato, A., Strandburg, K. J., Prinz, F. and Swendsen, R. H.: 1987, Why the brazil nuts

are on top: Size segregation of particulate matter by shaking, *Physical Review Letters* **58**(10), 1038.

Roufail, R., Klein, B. and Radziszewski, P.: 2012, Morphological Features and Discrete Element Method (Dem) Forces Produced in High Speed Stirred Mill, *XXVI International Mineral Processing Congress (IMPC) Proceedings. New Delhi, India.*

Roux, J.-N. and Combe, G.: 2003, On the meaning and microscopic origins of quasistatic deformation of granular materials, *16th ASCE Engineering Mechanics Conference*, Vol. 48, p. 56.

Roux, J. N.and Combe, G.: 2002, Quasistatic rheology and the oorigin of strain, *Comptes Rendus Physique* **3(2)**, 131–140.

Roux, S. and Radjai, F.: 1998, Texture-dependent rigid-plastic behavior, *Physics of dry granular media*, Springer, pp. 229–236.

Sano, O.: 2005, Dilatancy, buckling, and undulations on a vertically vibrating granular layer, *Physical Review E* **72**(5), 051302.

Savage, S. B.: 1984, The mechanics of repid flows, *Adv. Appl. Mech.* **24**, 289–366.

Savage, S. and Hutter, K.: 1998, The motion of a finite mass of granular material down a rough incline., *J. Fluid Mech* **199**, 177–215.

Shaviv, G.: 2004, Numerical experiments in screening theory, *Astronomy & Astrophysics* **418**(3), 801–811.

Shigeo, M.: 1960, Proposal of a new index for expressing the performance of screens, *Chemical Engineering* **24**(3), 150–155.

Shimosaka, A., Higashihara, S. and Hidaka, J.: 2000, Estimation of the sieving rate of powders using computer simulation, *Advanced Powder Technology* **11**(4), 487–502.

Shuyan, W., Xiang, L., Huilin, L., Long, Y., Dan, S., Yurong, H. and Yonglong: 2009, Numerical simulations of flow behavior of gas and particles in spouted beds using frfriction-kinetc ststress model, *Power Technology* **196**, 184–193.

Silbert, L. E., Ertaş, D., Grest, G. S., Halsey, T. C., Levine, D. and Plimpton, S. J.: 2001, Granular flow down an inclined plane: Bagnold scaling and rheology, *Physical Review E* **64**(5), 051302.

Silbert, L. E., Landry, J. W. and Grest, G. S.: 2003, Granular flow down a rough inclined plane: transition between thin and thick piles, *Physics of Fluids (1994-present)* **15**(1), 1–10.

Soldinger, M.: 1999, Interrelation of stratification and passage in the screening process, *Minerals Engineering* **12**(5), 497–516.

Soldinger, M.: 2000, Influence of particle size and bed thickness on the screening process, *Minerals engineering* **13**(3), 297–312.

Soldinger, M.: 2002, Transport velocity of a crushed rock material bed on a screen, *Minerals Engineering* **15**(1), 7–17.

Subasinghe, G., Schaap, W. and Kelly, E.: 1989, Modelling the screening process - an empirical approach, *Minerals Engineering* **2**(2), 235–244.

Subasinghe, G., Schaap, W. and Kelly, E.: 1990, Modelling screening as a conjugate rate process, *International Journal of Mineral Processing* **28**(3), 289–300.

Sultanbawa, F., Owens, W. and Pandiella, S.: 2001, A new approach to the prediction of particle separation by sieving in flour milling, *Food and bioproducts processing* **79**(4), 211–218.

Suzuki, T., Hotta, N. and Miyamoto, K.: 2003, Influence of riverbed roughness on debris flows, *J. Erosion Contr. Eng* **56**, 5–13.

Swinney, H. L. and Rericha, E.: 2004, Pattern formation and shocks in granular gases, *arXiv preprint cond-mat/0408252* .

Taberlet, N., Richard, P., Valance, A., Losert, W., Pasini, J. M., Jenkins, J. T. and R., D.: 2003, Superstable Granular Heap in a Thin Channel, *Physical Review Letters* **91(26)**, 264301.1–264301.5.

Takahashi, T.: 2009, A Review of Japanese Debris Flow Research, *International Journal of Erosion Control Engineering* **2(1)**, 1–14.

Tripathi, A. and Khakhar, D.: 2011, Rheology of binary granular mixtures in the dense flow regime, *Physics of Fluids (1994-present)* **23**(11), 113302.

Tsai, P. and Chang, T.: 2009, Effects of open trench siding on vibration-screening effectiveness using the two-dimensional boundary element method, *Soil Dynamics and Earthquake Engineering* **29**(5), 865–873.

Tsakalakis, K.: 2001, Some basic factors affecting scree performance in horizontal vibrating screens, *The European Journal of Mineral Processing and Environmental Protection, I* pp. 42–54.

Tsuji, Y., Kawaguchi, T. and Tanaka, T.: 1993, Discrete particle simulation of two-dimensional fluidized bed, *Powder Technology* **77**(1), 79–87.

Tunuguntla, D. R.: 2015, Polydisperse granular flows over inclined channels.

Tunuguntla, D. R., Thornton, A. R. and Weinhart, T.: 2015, From discrete elements to continuum fields: Extension to bidisperse systems, *Computational Particle Mechanics* pp. 1–17.

Van der Vaart, K., Gajjar, P., Epely-Chauvin, G., Andreini, N., Gray, J. and Ancey, C.: 2015, An underlying asymmetry within particle-size segregation, *arXiv preprint arXiv:1501.06879* .

Vidyapati, V., Langroudi, M. K., Sun, J., Sundaresan, S., Tardos, G. and Subramaniam, S.: 2012, Experimental and computational studies of dense granular flow: Transition from quasi-static to intermediate regime in a couette shear device, *Powder Technology* **220**, 7–14.

Vidyapati, V. and Subramaniam, S.: 2012, Granular rheology and phase transition: Dem simulations and order-parameter based constitutive model, *Chemical Engineering Science* **72**, 20–34.

Walton, O. R. and Braun, R. L.: 1986, Viscosity, granular-temperature, and stress calculations for shearing assemblies of inelastic, frictional disks, *Journal of Rheology* **30**(5), 949–980.

Warr, S., Huntley, J. M. and Jacques, G. T.: 1995, Fluidization of a two-dimensional granular system: Experimental study and scaling behavior, *Physical Review E* **52**(5), 5583.

Weinhart, T., Thornton, A. R., Luding, S. and Bokhove, O.: 2012, Closure relations for shallow granular flows from particle simulations, *Granular Matter* **14**(4), 531–552.

Whiten, W. and Herbst, J.: 1984, Models and control techniques for crushing plants, *Control 84, Minl. Metall. Process, AIME Annual Meeting, Los Angeles, USA*, pp. 217–225.

Whiten, W. and White, M.: 1979, Modelling and simulation of high tonnage crushing plants, *Proceedings of the 12th International Mineral Processing Congress, Sao Paulo, Brazil*, Vol. 2, pp. 148–158.

Williams, J.: 1963, The segregation of powders and granular materials, *Fuel Soc. J* **14**, 29–34.

Williams, J. C.: 1976, The segregation of particulate materials. a review, *Powder Technology* **15**(2), 245–251.

Wodzinski, P.: 2003, Screening of fine granular material, *Coal Preparation* **23**(4), 183–211.

Xiao, J. and Tong, X.: 2012, Particle stratification and penetration of a linear vibrating screen by the discrete element method, *International Journal of Mining Science and Technology* **22**(3), 357–362.

Yang, R., Yu, A., McElroy, L. and Bao, J.: 2008, Numerical simulation of particle dynamics in different flow regimes in a rotating drum, *Powder Technology* **188**(2), 170–177.

Yanhua, C. and Xin, T.: 2010, Modeling screening efficiency with vibrational parameters based on dem 3d simulation, *Mining Science and Technology (China)* **20**(4), 615–620.

Zhu, H. and Yu, A.: 2002, Averaging method of granular materials, *Physical Review E* **66**(2), 021302.

Zhu, H., Zhou, Z., Yang, R. and Yu, A.: 2007, Discrete particle simulation of particulate systems: theoretical developments, *Chemical Engineering Science* **62**(13), 3378–3396.